

Coarse graining and control theory model reduction

David E. Reynolds ¹

ABSTRACT: We explain a method, inspired by control theory model reduction and interpolation theory, that rigorously establishes the types of coarse graining that are appropriate for systems with quadratic, generalized Hamiltonians. For such systems, general conditions are given that establish when local coarse grainings should be valid. Interestingly, our analysis provides a reduction method that is valid regardless of whether or not the system is isotropic. We provide the linear harmonic chain as a prototypical example. Additionally, these reduction techniques are based on the dynamic response of the system, and hence are also applicable to nonequilibrium systems.

KEY WORDS: coarse graining; control theory; model reduction; Hankel operator; operator theory

¹Department of Physics, University of California, Santa Barbara, CA 93106

1 Introduction

Despite many of the great successes of statistical mechanics, it still lacks adequate methods for systematically treating heterogeneous and nonequilibrium systems. This is especially disconcerting considering that much of the world about us is both heterogeneous and far from equilibrium. In addition, the treatment of open systems and systems with nontrivial boundary conditions have yet to be systematically incorporated into statistical mechanics². It is not the purpose of this paper to address all of these deficiencies. Rather, we introduce techniques from control theory engineering and interpolation theory to shed new light on such problems.

It is a standard practice in physics to simplify complicated systems. In particular limits, such as high-temperature or low-density, these idealizations may become exact. We will discuss two of the main methods used in physics to construct reduced-order models.

The projection-operator formalism (POF) of Mori and Zwanzig [6, 7, 5, 12] is a method from nonequilibrium statistical mechanics. It allows contact between the constitutive conservative microscopic equations and the more macroscopic phenomenological Langevin equations. The key mathematical ingredient in this approach, given an arbitrary observable, is to project along particular “directions” in state space in order to obtain an alternative evolution equation involving contributions from a forcing term and from a memory kernel. Here the projections involved are simply integrations over the appropriate phase space variables. A textbook application of the POF is a particle in a heat bath [5, 8, 13, 2]. In this example, there is a clear split between important (system) variables and the less important (environment) variables. Thus, taking the system variables as the particle’s position and momentum justifies projecting out the bath variables.

The renormalization group (RG) from field theory and equilibrium statistical mechanics [33, 34], in its original form, involves identifying how the physics of a system changes with scale. Equivalently, the renormalization group identifies how the parameters of a system’s Hamiltonian or Lagrangian vary as the system is coarse grained. In the RG, systems are, almost invariably, locally coarse grained (i.e. locally-averaged). In the context of equilibrium statistical mechanics, the coarse graining is realized with the appropriate partial trace of a Boltzmann weight. Formally, the partial trace is equivalent to the projections used in the POF.

An important observation is that both the POF and RG are completely general techniques. Although typical system reductions are either based on *a priori* system-environment splits or obvious symmetries dictating local coarse graining, there is enormous ambiguity in choosing which states to

²Of course the latter concern is somewhat atypical considering that boundary terms are usually deemed unimportant in the thermodynamic limit.

trace out ³. Intuition is enough of a guide for determining how to coarse grain homogeneous systems with local interactions. However, without some direction for dealing with heterogeneous systems, possibly with nonlocal interactions, the POF and RG are too general; they are useless. For instance, locally averaging about the interface in a layered system loses important information about the system. Additionally, locally averaging such systems is actually more likely to complicate the model. Complications arise since the averaged theory would pick up extra couplings to enforce the constraint of well-defined boundaries and induce couplings between the bulk of the different layers. In short, for general systems, local coarse graining is likely to discard important details. Consequently, as the effective influence of these discarded details is reincorporated into the coarsened description of the system, the new effective theory becomes increasingly complicated.

The above considerations support the view advocated in the work by Bricmont and Kupiainen [37, 36, 35]. They contend that systems should not be blindly coarse grained scale by scale, but rather, large fluctuations should remain fixed while those degrees of freedom corresponding to small fluctuations are integrated away. A direct consequence of this perspective is that nonlocal coarse graining is on the same footing as its local counterpart. Intuitively, internal states that cause the largest fluctuations are the most relevant. The problem with such a program is that there exists no general framework that allows for an unambiguous measure of the relative importance of a system's internal degrees of freedom.

It is our claim that methods from control theory and modern interpolation theory provide a complete, general framework for determining how to appropriately coarse grain linear and linearly-dominated nonlinear systems. Consequently, this opens up many new possible avenues to address the full nonlinear problem [27, 28, 29]. The primary idea of this approach is to coarse grain a system based on its dynamic response. For linear systems, it is possible to develop a completely unambiguous measure of how the internal states of a system contribute to the response. In other words, it is possible to assign a relative importance to the internal degrees of freedom. Determining this measure then dictates how the system should be coarse grained. An especially nice feature of the control theory analysis is that it decomposes the response into two separate, physically intuitive, parts: the controllability and observability of the internal states. Furthermore, these techniques are not limited to the idealized setting in which all of the internal degrees of freedom of the system can be perfectly measured. In fact, these methods were tailored to deal with physical systems in an ex-

³Taking the partial trace of the probability density (Boltzmann weight) produces the probability density for the corresponding random variable. Thus, the only real constraint one should put on the partial trace is that it corresponds to a measurable random variable.

perimental setting! They are applicable even if the actuators and sensors interfaced with the system are imperfect. These methods are not only of great theoretical use; they are of practical use as well.

In work by Hartle and Brun [10], it is speculated that local coarse graining produces more deterministic effective equations of motion than nonlocal coarse graining. The problem with this claim is that it was made based on investigating the homogeneous linear harmonic chain on \mathbb{Z}_N (i.e. on a ring) and considering a set of measure zero of all possible ways to coarse grain the system. The main result of our paper rigorously establishes for what (linear) systems the above claim is true and how it breaks down for general linear systems. A primary instance when it breaks down is for heterogeneous systems. We also establish how to appropriately coarse grain systems when local coarse graining breaks down.

This paper serves two functions; (1) to introduce and integrate basic concepts from control theory into standard physics problems, and (2) to develop and apply a new algorithm for coarse graining that complements existing physical reduction techniques. In Section 2 we provide background material on the open loop control of linear systems. The definitions of controllability and observability are made precise. The controllability and observability operators and gramians are then introduced. From these objects, we establish a simultaneous measure of controllability and observability. This measure specifies the relative importance of different internal degrees of freedom. It also dictates how to model reduce or, equivalently, to coarse grain. Appendix A contains important details that generalize the control theory model reduction techniques in Section 2 to conservative and unstable systems. The lower bound in Appendix A is a new result. Lastly, in Section 3, we apply model reduction techniques to oscillator systems to determine the “natural” reductions they admit. We see that under some circumstances, depending on the spectral content of the system, local coarse graining is valid. We also show how to coarse grain a system even if it is not homogeneous and isotropic. Local coarse graining cannot be expected to be appropriate for general quadratic Hamiltonians. In fact, our analysis shows the precise manner in which it is not. For illustrative purposes, we examine the linear harmonic chain in detail.

2 A control theory tutorial

This section describes how control theory methods, in particular Hankel norm analysis, may be used to determine the relative importance of the internal degrees of freedom for arbitrary linear systems. A state’s importance is directly related to its contribution to the system’s response. In this section, we introduce the requisite control theory terminology and notation

that will be used throughout.

In the opening subsection, we introduce the linear systems under investigation, their corresponding input-output behavior (response), and some requisite material on the realization theory of input-output operators. In the next subsection, we provide definitions and measures of controllability and observability. The Hankel operator, its interpretation in terms of controllability and observability, and its relation to balanced realizations comprise the final subsection. The latter topics are especially important in control theory model reduction and, consequently, also for coarse graining. Although we made no attempt for this tutorial to be an exhaustive review, we include enough detail for the paper to be self-contained. All theorems in this section are stated without proof. The interested reader is encouraged to consult the following references [20, 24, 15, 16, 25]. Those who are already familiar with the above concepts may comfortably skip ahead to Section 3.

2.1 Linear Systems and Realizations

This paper concerns linear time invariant (LTI) systems (i.e. linear systems with time translation invariance) of the form:

$$\begin{aligned} \dot{x} &= \mathbf{A}x + \mathbf{B}u \\ y &= \mathbf{C}x + \mathbf{D}u \end{aligned} \quad , \quad \begin{cases} t \geq t_0, \\ x(t) \in \mathbb{R}^n, \\ u(t) \in \mathbb{R}^m, \\ y(t) \in \mathbb{R}^p, \end{cases} \quad (1)$$

where x is the “internal” state of the system, y represents quantities directly measured by appropriately positioned sensors, and u represents the external driving force. The matrix \mathbf{A} captures the natural dynamics of the system, while, respectively, \mathbf{B} and \mathbf{C} dictate which internal states of the system are in contact with the driving and measurement. \mathbf{D} is responsible for the feedthrough of the system. Feedthrough is the (possibly amplified) contribution of the driving that is directly measured. A control theoretic diagram representing this system is in Figure 1. Expressing the system in this form reflects that only partial information is measured and that the system is open. Since the system is LTI, \mathbf{A} , \mathbf{B} , \mathbf{C} , and \mathbf{D} are constant coefficient matrices.

The general solution to the above problem is given by:

$$y(t) = \underbrace{\mathbf{C}e^{\mathbf{A}(t-t_0)}x_0}_{\text{zero input response}} + \underbrace{\int_{t_0}^t \mathbf{C}e^{\mathbf{A}(t-\tau)}\mathbf{B}u(\tau)d\tau}_{\text{zero state response}} + \underbrace{\mathbf{D}u(t)}_{\text{feedthrough}} \quad (2)$$

If we consider only the zero state response (trivial initial conditions), then

$$y = Gu$$

$$= \int \mathcal{K}(t, \tau)u(\tau)d\tau = \int_{t_0}^t \mathbf{C}e^{\mathbf{A}(t-\tau)}\mathbf{B}u(\tau)d\tau. \quad (3)$$

The integral kernel has many names. In the time domain it is referred to as the impulse response or the Green's function. Alternatively, for stable, LTI systems, the Fourier transform of the integral kernel is also known as the transfer matrix, Green's function in the frequency domain, or the propagator. Since feedthrough is not crucial in our analysis, $\mathbf{D} = 0$ from this point forward.

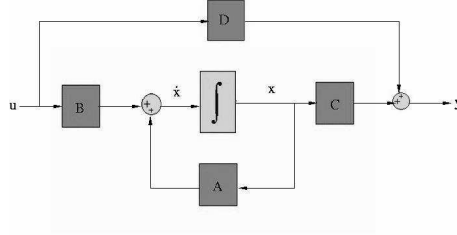


Figure 1: A block diagram representation of the linear system from 1 and 2. Directed lines flowing into boxes represents vectors being multiplied by operators (or matrices). For instance, initially u flows into \mathbf{B} , hence the output of the first box is $\mathbf{B}u$. The circles in the diagram are adders. Vectors that flow into adders are summed.

In control theory, a system is specified by an experiment. This is reflected by the dependence of G on \mathbf{B}, \mathbf{C} , and \mathbf{D} . A system is defined by its response (i.e. by G). From an experiment, the only available data is from the inputs and outputs. Hence, the matrices $(\mathbf{A}, \mathbf{B}, \mathbf{C}, \mathbf{D})$ are unknown. Constructing all of such matrices corresponding to a given response is the objective of realization theory. The system matrices $(\mathbf{A}, \mathbf{B}, \mathbf{C}, \mathbf{D})$ form a state space realization of the system. For a given system, there does not exist a unique realization. However, given a realization, there exists a unique system. The choice of experiment fixes the system's inputs and outputs. The remaining ambiguity is due to the internal states of the system. For instance, an arbitrary invertible, linear change of variables, $x = \mathbf{R}z$, demonstrates this. $(\mathbf{R}^{-1}\mathbf{A}\mathbf{R}, \mathbf{R}^{-1}\mathbf{B}, \mathbf{C}\mathbf{R}, \mathbf{D})$ is also a realization of G . Since G is invariant under the above similarity transformations, realizations belong to equivalence classes. The remaining indeterminateness arises since there is not a bound on the number of internal degrees of freedom. In fact, there may be arbitrarily many internal states that do not contribute to the system's response. State space realizations that have the minimal internal state dimension are called minimal realizations

⁴. Although G is typically an infinite rank operator (i.e. the image of G is infinite dimensional), the internal state dimension of its minimal realizations gives it an order. When the minimal realization is stable, the order of G is also known as its McMillan degree.

Minimal realizations represent the part of the system that is observable and controllable. To clarify this, we will introduce the definitions of controllability and observability. We then define the controllability and observability operators along with their respective gramians. These concepts are imperative to assigning a measure of how much an individual internal state contributes to the system's response.

2.2 Controllability and Observability

• Controllability

Controllability concerns the effects of driving on the system. In particular, a system is controllable if it is possible to drive a system from any initial configuration to any final configuration. An internal state of a system is considered uncontrollable if it cannot be driven to every other state.

The issue of whether or not a system (or state) is controllable is a yes-or-no question. However, we may still intuitively assign a degree of controllability to a state. An example of this is to consider the response of a conservative system when it is driven at one of its characteristic frequencies (at resonance). This is mathematically realized by a divergence (or a peak, in general) in the Fourier transform of the response. This is the simplest example of a system's mode being very controllable, insofar that we can elicit a large response from small amplitude driving⁵. It is easy to drive states in the direction of this mode. Generally input-output resonances do not always correspond to internal resonances. Should there be a set or subspace of state or phase space that can not be reached via driving, then such "directions" are uncontrollable. A system is controllable if every direction in state or phase space is controllable. The following provides a more formal and precise definition of controllability.

Definition 2.2.1 A system is controllable if it is possible to drive any initial state x_0 to any final state x_f in any nonzero time interval.

• Observability

Observability describes how easily the internal state of the system can be reconstructed from measurements of the output. Intimately connected

⁴Minimal realizations of a given state dimension all belong to the same equivalence class.

⁵Driving with small amplitude is also termed driving or forcing with small gain.

to this is the precise determination of the internal initial conditions. Initial conditions that cannot be reconstructed are the system's unobservable states.

The mechanical model of a particle in a heat bath provides a physical example of observable versus unobservable states. As alluded to earlier, such as system admits a natural system-environment split. In this case the system is the single oscillator, while the environment is the bath. The oscillator is the primary object under investigation and hence, an experimental apparatus is devised to measure its displacement and/or velocity. Since the bath is composed of innumerable constituent particles (or oscillators), the individual trajectories of the bath particles are unknown. While the single oscillator is strongly observable, the bath is only weakly observable. It is possible to reconstruct the initial conditions for the single oscillator but not for the entire bath. A more precise and formal definition of observability is:

Definition 2.2.2 A system is observable if it is possible to fully determine any initial state x_0 by measuring y over any nonzero time interval.

• **Controllability and observability operators**

It is clear that the input-output operator, G , from equation (3) takes in inputs from u from some space and outputs y in another. For concreteness, from now on we will consider the domain of G to be $\mathcal{L}_2^m[-T, T]$ (i.e. m copies of \mathcal{L}_2) and the range to be $\mathcal{L}_2^p[-T, T]$. More generally, u may also be a vector in \mathcal{L}_1^m , \mathcal{L}_∞^m , or a Langevin contribution to the dynamics. The construction of the controllability and observability operators, Ψ_c and Ψ_o respectively, is largely motivated by the fact that the Hankel operator, to be introduced later, can be factored into their product. Thus, the response may be decomposed into observability and controllability.

The controllability operator is defined by:

$$\Psi_c : \mathcal{L}_2^m[-T, 0] \rightarrow \mathbb{R}^n \quad (4)$$

$$\Psi_c u = \int_{-T}^0 e^{-\mathbf{A}\tau} \mathbf{B}u(\tau) d\tau = \int_0^T e^{\mathbf{A}\tau} \mathbf{B}u(-\tau) d\tau$$

Formally Ψ_c is not defined on the full domain of G . It can be extended to the full space, however, by defining $\mathcal{L}_2^m[0, T]$ to be in its null space. The controllability operator allows for an algebraic definition of controllability.

Theorem 2.2.3 A linear system, as in equation (1), specified by $(\mathbf{A}, \mathbf{B}, \mathbf{C}, \mathbf{D})$ is controllable if and only if the image of Ψ_c is all of \mathbb{R}^n .

If a system in equation (1) is controllable, we call the system pair (\mathbf{A}, \mathbf{B}) controllable. Additionally, the space of states that are controllable forms

an \mathbf{A} -invariant subspace. The controllable subspace is precisely the image of Ψ_c , $\mathcal{R}(\Psi_c)$.

Similarly, the observability operator is defined by:

$$\begin{aligned}\Psi_o : \mathbb{R}^n &\rightarrow \mathcal{L}_2^p[0, T] \\ \Psi_o z &= \mathbf{C}e^{\mathbf{A}t}z\end{aligned}\tag{5}$$

In contrast to controllability, the set of observable states do not form an invariant subspace. The span of the unobservable states forms an \mathbf{A} -invariant subspace⁶. The null space of Ψ_o , $Null(\Psi_o)$, comprises the unobservable subspace. This implies that a system is observable provided that Ψ_o has full rank (i.e. the null space is empty). This gives the formal algebraic definition of observability.

Theorem 2.2.4 (Test for observability) A linear system given by (1) is observable iff $\text{rank}(\Psi_o) = n$ (i.e. Ψ_o has full rank).

If a system is observable, we call the system pair (\mathbf{C}, \mathbf{A}) observable. Controllability and observability are completely dual to each other. For example, (\mathbf{A}, \mathbf{B}) is controllable if and only if $(\mathbf{B}^\dagger, \mathbf{A}^\dagger)$ is observable.

• **Controllability and observability gramians**

Superficially it may seem that the above operators only give us limited information. Specifically, we only have binary tests for controllability and observability based on whether or not the state is in $\mathcal{R}(\Psi_c)$ or in $Null(\Psi_o)$. Our objective is to determine how observable and controllable a state is in order to quantify its contribution to the response. It is precisely the controllability and observability gramians that provide this information. However, as will soon become apparent, the operators are intimately related to the gramians.

Determining $\mathcal{R}(\Psi_c)$ and $Null(\Psi_o)$ is a formidable challenge since the domain of Ψ_c and the range of Ψ_o are infinite dimensional spaces. However, the formal operator adjoint makes the problem more tractable. Since $\Psi_c : \mathcal{L}_2^m[-T, 0] \rightarrow \mathbb{R}^n$ this then implies that $\Psi_c^\dagger : \mathbb{R}^n \rightarrow \mathcal{L}_2^m[-T, 0]$, where Ψ_c^\dagger is the operator adjoint of Ψ_c . Similarly, $\Psi_o^\dagger : \mathcal{L}_2^p[0, T] \rightarrow \mathbb{R}^n$. An important property of the adjoint of an operator is that its image is perpendicular to the original operator's null space, that is $\mathcal{R}(\Psi_c^\dagger) \perp Null(\Psi_c)$. Also $\mathcal{R}(\Psi_c^\dagger) \perp Null(\Psi_c)$ and $Null(\Psi_o) \perp \mathcal{R}(\Psi_o^\dagger)$. Consequently, $\mathcal{R}(\Psi_c) = \mathcal{R}(\Psi_c \Psi_c^\dagger)$ and $Null(\Psi_o) = Null(\Psi_o^\dagger \Psi_o)$. However, since Ψ_c^\dagger maps \mathbb{R}^n to $\mathcal{L}_2^m[-T, 0]$ and Ψ_o^\dagger maps $\mathcal{L}_2^p[0, T]$ to \mathbb{R}^n , $\Psi_c \Psi_c^\dagger$ and $\Psi_o^\dagger \Psi_o$ are $n \times n$ matrices. Finding the controllability and observability subspaces reduces to discovering the images and null spaces of $n \times n$ matrices.

⁶This and its controllable analog are important because they are responsible for the Kalman decomposition.

From the definition of the adjoint, the expression for Ψ_c^\dagger is

$$\begin{aligned} \Psi_c^\dagger &: \mathbb{R}^n \rightarrow \mathcal{L}_2^m[-T, 0], \\ \Psi_c^\dagger z &= \mathbf{B}^\dagger e^{-\mathbf{A}^\dagger t} z \quad \text{For all } z \in \mathbb{R}^n, t \in [-T, 0]. \end{aligned} \quad (6)$$

The following relation holds for Ψ_o^\dagger :

$$\begin{aligned} \Psi_o^\dagger &: \mathcal{L}_2^p[0, T] \rightarrow \mathbb{R}^n, \\ \Psi_o^\dagger f &= \int_0^T e^{\mathbf{A}^\dagger \tau} \mathbf{C}^\dagger f(\tau) d\tau. \end{aligned} \quad (7)$$

From above, we are left with objects that are of fundamental importance for establishing quantitative measures of controllability and observability, the gramians. The controllability gramian, \mathbf{W}_c , is defined by:

$$\begin{aligned} \mathbf{W}_c(T) &= \Psi_c \Psi_c^\dagger \\ &= \int_0^T e^{\mathbf{A}t} \mathbf{B} \mathbf{B}^\dagger e^{\mathbf{A}^\dagger t} dt. \end{aligned} \quad (8)$$

The observability gramian, \mathbf{W}_o , is defined by:

$$\begin{aligned} \mathbf{W}_o(T) &= \Psi_o^\dagger \Psi_o \\ &= \int_0^T e^{\mathbf{A}^\dagger t} \mathbf{C}^\dagger \mathbf{C} e^{\mathbf{A}t} dt. \end{aligned} \quad (9)$$

From their definitions, the gramians are both self-adjoint and positive semi-definite. Additionally, the controllable subspace of the system is the image of $\mathbf{W}_c(T)$. Thus, a linear system is controllable if and only if $\mathbf{W}_c(T)$ is nonsingular (invertible). Similarly, the unobservability subspace is the null space of $\mathbf{W}_o(T)$. A linear system is then observable if and only if $\mathbf{W}_o(T)$ is nonsingular (i.e. the null space is empty). Consequently, controllability and observability are determined by calculating two matrices, $\mathbf{W}_c(T)$ and $\mathbf{W}_o(T)$. Equations (8) and (9) are computationally not very useful. It is typically easier to determine the gramians from the equations that they satisfy.

$$\frac{d\mathbf{W}_c}{dT} = \mathbf{A} \mathbf{W}_c + \mathbf{W}_c \mathbf{A}^\dagger + \mathbf{B} \mathbf{B}^\dagger; \quad \mathbf{W}_c(0) = 0 \quad (10)$$

$$\frac{d\mathbf{W}_o}{dT} = \mathbf{A}^\dagger \mathbf{W}_o + \mathbf{W}_o \mathbf{A} + \mathbf{C}^\dagger \mathbf{C}; \quad \mathbf{W}_o(0) = 0 \quad (11)$$

For stable systems, in the limit as $T \rightarrow \infty$, the gramians satisfy algebraic Lyapunov equations ⁷.

⁷The Lyapunov equations are $\mathbf{A} \mathbf{W}_c + \mathbf{W}_c \mathbf{A}^\dagger + \mathbf{B} \mathbf{B}^\dagger = 0$ and $\mathbf{A}^\dagger \mathbf{W}_o + \mathbf{W}_o \mathbf{A} + \mathbf{C}^\dagger \mathbf{C} = 0$.

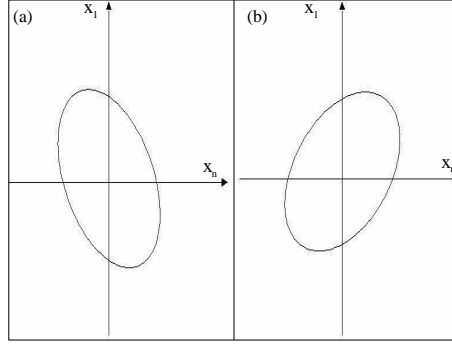


Figure 2: (a) depicts a controllability ellipsoid, while (b) depicts an observability ellipsoid. The semimajor axis of the ellipsoid in (a) indicates the most controllable direction in state space, and for the ellipsoid in (b) it indicates the most observable direction.

The directions in state or phase space corresponding to trivial eigenvalues of \mathbf{W}_c are uncontrollable. Therefore, the eigenvectors of \mathbf{W}_c corresponding to small eigenvalues are only weakly controllable. It is along those directions that the controllability gramian is almost singular. Physically, it requires much higher gains to reach these states than the more controllable states. More precisely, consider the quadratic energy functional $F(u) = \int_{-T}^0 \|u(t)\|_{\mathbb{R}^m}^2 dt = \|u\|_{\mathcal{L}_2^m[-T,0]}^2$ that measures the energy due to driving. The u that expends the least energy to reach a state $\bar{x} \in \mathbb{R}^n$ from the origin ⁸ is given by $u_{min} = \Psi_c^\dagger \mathbf{W}_c^{-1} \bar{x}$. The energy due to such driving is

$$\begin{aligned}
\|u_{min}\|_{\mathcal{L}_2^m[-T,0]}^2 &= \langle u_{min}, u_{min} \rangle_{\mathcal{L}_2^m} \\
&= \langle \Psi_c^\dagger \mathbf{W}_c^{-1} \bar{x}, \Psi_c^\dagger \mathbf{W}_c^{-1} \bar{x} \rangle_{\mathcal{L}_2^m} \\
&= \langle \bar{x}, \mathbf{W}_c^{-1} \Psi_c \Psi_c^\dagger \mathbf{W}_c^{-1} \bar{x} \rangle_{\mathbb{R}^n} = \langle \bar{x}, \mathbf{W}_c^{-1} \bar{x} \rangle_{\mathbb{R}^n} \\
&= \|\mathbf{W}_c^{-1/2} \bar{x}\|_{\mathbb{R}^n}^2.
\end{aligned} \tag{12}$$

If we drive the system in state or phase space with minimal force $\|u_{min}\|^2 \leq 1$, the corresponding region in state or phase space is a solid ellipsoid in \mathbb{R}^n . This set, depicted in Figure 2(a), corresponds to $\{\bar{x} \in \mathbb{R}^n : \bar{x}^\dagger \mathbf{W}_c^{-1} \bar{x} \leq 1\}$. This ellipsoid is also specified by $\{\bar{x} \in \mathbb{R}^n : \bar{x} = \mathbf{W}_c^{1/2} z, \|z\|_{\mathbb{R}^n} \leq 1\}$. While $\|\mathbf{W}_c^{-1/2} \bar{x}\|^2$ measures energy expenditure, $\frac{\|\mathbf{W}_c^{-1/2} \bar{x}\|^2}{\|\bar{x}\|^2} = \frac{\bar{x}^\dagger \mathbf{W}_c \bar{x}}{\bar{x}^\dagger \bar{x}}$ measures a state's controllability. This confirms the intuition that states corresponding to small eigenvalues of \mathbf{W}_c are the least controllable.

Physically, the observability operator produces a response given an

⁸This is provided that the system is controllable and the dynamics of the system are restricted to satisfy (1) with $\mathbf{D} = 0$.

initial condition. What does this reveal about the inverse problem of reconstructing the initial conditions from measurements of the system's response? Mathematically this problem is posed as determining

$$\min_{\bar{x} \in \mathbb{R}^n} \|y - \Psi_o \bar{x}\|_{\mathcal{L}_2^p[0,T]}^2.$$

When y is in the image of Ψ_o , it is possible to precisely specify the initial conditions, \bar{x} . Otherwise, the initial condition minimizing $\|y - \Psi_o \bar{x}\|_{\mathcal{L}_2^p[0,T]}^2$, given an arbitrary $y \in \mathcal{L}_2^p[0,T]$, is $\bar{x}_{opt} = \mathbf{W}_o^{-1} \Psi_o^\dagger y$. In order to obtain a quantitative measure of observability, we need only consider the outputs, $y = \Psi_o \bar{x}$. Immediately we recognize that $\|y\|_{\mathcal{L}_2^p[0,T]}^2 / \|\bar{x}\|_{\mathbb{R}^n}^2 = \|\mathbf{W}_o^{1/2} \bar{x}\|_{\mathbb{R}^n}^2 |_{\|\bar{x}\| \leq 1}$ measures a state's observability. For instance, initial conditions, \bar{x} , corresponding to small eigenvalues of \mathbf{W}_o elicit smaller responses than other states and, consequently, are less observable. If noise is present, responses resulting from such initial conditions would not be observed at all. The set $\{\bar{x} \in \mathbb{R}^n : \bar{x} = \mathbf{W}_o^{1/2} z, \|z\|_{\mathbb{R}^n} \leq 1\}$ corresponds to the observability ellipsoid depicted in Figure 2(b). The directions along which the ellipsoid is long are the most observable.

The utility in considering controllability and observability separately is that they have precise and experimentally relevant interpretations. A problem with this approach is that it initially obstructs the path to ascribing measures of response to physical states. For instance, it is possible to model reduce based on either controllability or observability⁹. Unfortunately, the measures of controllability and observability are not unique. This is transparent after considering how \mathbf{W}_o and \mathbf{W}_c transform under similarity transformations to the system. \mathbf{W}_o transforms as $\mathbf{W}_o \xrightarrow{\mathbf{R}} \tilde{\mathbf{W}}_o = \mathbf{R}^\dagger \mathbf{W}_o \mathbf{R}$, while \mathbf{W}_c transforms as $\mathbf{W}_c \xrightarrow{\mathbf{R}} \tilde{\mathbf{W}}_c = \mathbf{R}^{-1} \mathbf{W}_c (\mathbf{R}^\dagger)^{-1}$. Thus, the gramians are not invariant under an arbitrary linear coordinate transformation. However, $\mathbf{W}_c \mathbf{W}_o$ transforms as $\mathbf{W}_c \mathbf{W}_o \xrightarrow{\mathbf{R}} \tilde{\mathbf{W}}_c \tilde{\mathbf{W}}_o = \mathbf{R}^{-1} \mathbf{W}_c \mathbf{W}_o \mathbf{R}$ under a similarity transformation of the system. The eigenvalues of $\mathbf{W}_c \mathbf{W}_o$ are invariants of the system, are intimately related to the Hankel operator of the system, and thus will prove invaluable for producing reduced-order models.

2.3 The Hankel Operator, Balanced Realizations, and Model Reduction

The theory of model reduction is closely related to that of system realizations. In model reduction, the goal is to find realizations (i.e. the matrices

⁹It has been shown in [4] that reductions based on the proper orthogonal decomposition (POD) is essentially equivalent to model reducing based on controllability.

(**A, B, C, D**) with minimal state dimension that approximately capture the system's input-output characteristics. Often being “near” the original system is enough to dramatically reduce the number of internal states needed to model the system. Here distance or “nearness” is defined by the standard induced-operator norm. For example, given an operator S that acts on \mathcal{L}_2 , the induced norm takes the form $\|S\|_{\mathcal{L}_2,i} = \sup_{\|v\|_{\mathcal{L}_2} \leq 1} \|Sv\|_{\mathcal{L}_2}$, where v is a vector in \mathcal{L}_2 . Also, supposing that \tilde{S} approximates S , we will be considering two measures of the error, the absolute error $\|S - \tilde{S}\|_{\mathcal{L}_2,i}$ and the relative error $\|S - \tilde{S}\|_{\mathcal{L}_2,i} / \|S\|_{\mathcal{L}_2,i}$. The relative error is more appropriate for unbounded operators, since most approximations are asymptotic estimates. The relative error is also the noise-to-signal ratio.

It is useful to note that there is an explicit expression for the induced \mathcal{L}_2 norm for bounded (stable), LTI, causal operators. Such operators are in the space \mathcal{H}_∞ . The primary difficulty with this formula is that it is difficult to use both numerically and analytically. To motivate the formula, recall that an arbitrary $m \times n$ matrix \mathbf{M} can be decomposed as $\mathbf{M} = \mathbf{U}\mathbf{\Sigma}\mathbf{V}^\dagger$ (i.e. the singular value decomposition) where \mathbf{U} and \mathbf{V} are respectively $m \times m$ and $n \times n$ unitary matrices and $\mathbf{\Sigma}$ is only nontrivial along the diagonal. The diagonal values $\Sigma_{ii} = \sigma_i(\mathbf{M}) \geq 0$ are called the singular values of \mathbf{M} . If $m > n$ then the singular values are the eigenvalues of $\sqrt{\mathbf{M}^\dagger\mathbf{M}}$, otherwise they are the eigenvalues of $\sqrt{\mathbf{M}\mathbf{M}^\dagger}$. Here $\|\mathbf{M}\|_{C^m,i} = \sigma_{\max}(\mathbf{M})$ where $\sigma_{\max}(\mathbf{M}) = \max_j \sigma_j(\mathbf{M})$ (i.e. the largest singular value). For a bounded, LTI, causal operator S such that $S(u) = \int_{-\infty}^t \mathcal{K}_S(t - \tau)u(\tau)d\tau$, $\|S\|_{\mathcal{L}_2,i} = \sup_{\omega \in \mathbb{R}} \sigma_{\max}(\hat{\mathcal{K}}_S(\omega))$ where $\hat{\mathcal{K}}_S(\omega)$ is the Fourier transform of $\mathcal{K}_S(t)$.

Coarse graining and model reduction are intimately related. While both are reduction methods, coarse graining emphasizes the spatial nature of reductions. Model reduction, as it will be presented here, emphasizes input-output resonances and approximating the response. Our approach to coarse graining is to identify the best way to model reduce, based on the response, and then ascertain the spatial structure of the reduction. The latter topic is elaborated upon for linear oscillator systems in the next section. Unfortunately, the former issue is a mathematically unresolved problem. The control/interpolation theoretic statement of this problem for stable systems (in the induced \mathcal{L}_2 -norm) is called the \mathcal{H}_∞ model reduction problem.

Definition 2.3.1 (\mathcal{H}_∞ Model Reduction Problem) Given a bounded, LTI, causal operator G of McMillan degree n , such that $G : \mathcal{L}_2 \rightarrow \mathcal{L}_2$, find $\inf_{\deg(\tilde{G}) \leq k} \|G - \tilde{G}\|_{\mathcal{L}_2,i}$ for \tilde{G} a bounded, LTI, causal operator and $k < n$.

Fortunately, enough is known about a related problem, the Hankel norm model reduction problem, to provide error bounds to the above \mathcal{H}_∞ prob-

lem. By using results from Hankel operator analysis and Hankel norm model reduction, we will be able to deduce physically-important results about coarse graining.

• **The Hankel operator**

The input-output picture corresponds to an experimental situation, albeit a complicated one. The full input-output operator, G , from $y = Gu$ represents continuously driving and measuring a system. This operator is difficult to study because it does not separate observation from driving. As will become apparent, the Hankel operator is the part of the input-output operator where the operations of measurement and forcing are separated.

To facilitate analysis, it is convenient to decompose $\mathcal{L}_2[-T, T]$ into $\mathcal{L}_2[-T, 0] \oplus \mathcal{L}_2[0, T]$, in other words, a causal (analytic) decomposition. LTI causal systems can be visualized in the following way:

$$\begin{bmatrix} y_- \\ y_+ \end{bmatrix} = \begin{bmatrix} G_{11} & G_{12} \\ G_{21} & G_{22} \end{bmatrix} \begin{bmatrix} u_- \\ u_+ \end{bmatrix} = \begin{bmatrix} \mathcal{T}_G & 0 \\ \Gamma_G & \tilde{\mathcal{T}}_G \end{bmatrix} \begin{bmatrix} u_- \\ u_+ \end{bmatrix}, \quad (13)$$

$$\begin{cases} y_+ \in \mathcal{L}_2^p[0, T], \\ y_- \in \mathcal{L}_2^p[-T, 0], \\ u_+ \in \mathcal{L}_2^m[0, T], \\ u_- \in \mathcal{L}_2^m[-T, 0]. \end{cases}$$

Causality implies that $G_{12} = 0$. The additional constraint that the system is LTI implies that $\mathcal{K}(t, \tau)$ is purely a function of $t - \tau$. \mathcal{T}_G and $\tilde{\mathcal{T}}_G$ are Toeplitz operators, while Γ_G is a Hankel operator. It is not vital nor required for the reader to be familiar with Hankel or Toeplitz operators. The interested reader is encouraged to consult [17, 18, 19, 21, 22, 23, 15, 16] to learn more about these operators. If we denote the projection operator onto $\mathcal{L}_2[0, T]$ by P_+ , then $P_+^2 = P_+$ and $\Gamma_G = P_+ G|_{\mathcal{L}_2[-T, 0]}$. Since such projection operators can never increase the norm, it follows that $\|\Gamma_G\| \leq \|G\|$. Similarly, $\|\mathcal{T}_G\| = \|\tilde{\mathcal{T}}_G\| \leq \|G\|$, where the first equality arises since \mathcal{T}_G and $\tilde{\mathcal{T}}_G$ differ only by time reversal. A somewhat surprising fact is that $\|\mathcal{T}_G\| = \|G\|$ [17]. Model reduction based on \mathcal{T}_G is equivalent to the full \mathcal{H}_∞ problem for stable systems. Unfortunately, the experiments represented by \mathcal{T}_G involve simultaneously driving and observing.

The Hankel operator, Γ_G , accepts inputs driving the internal state to some x_0 at time $t = 0$. Subsequently, the system is measured as it evolves in time. The separation of driving and measurement allows for Γ_G to be factored in the particularly convenient way:

$$\begin{aligned} \Gamma_G(u) &= P_+ G|_{\mathcal{L}_2[-T, 0]} u = P_+ \int_{-T}^0 \mathbf{C} e^{\mathbf{A}(t-\tau)} \mathbf{B} u(\tau) d\tau \\ &= P_+ \mathbf{C} e^{\mathbf{A}t} \int_{-T}^0 e^{-\mathbf{A}\tau} \mathbf{B} u(\tau) d\tau = \Psi_o \Psi_c u. \end{aligned} \quad (14)$$

The Hankel operator may be factored as a product of the observability

operator and controllability operator: $\Gamma_G = \Psi_o \Psi_c$. It follows that

$$\begin{aligned}
\|\Gamma_G\|_{\mathcal{L}_{2,i}}^2 &= \|\Gamma_G^\dagger \Gamma_G\|_{\mathcal{L}_{2,i}} \\
&= \|\Psi_c^\dagger \Psi_o^\dagger \Psi_o \Psi_c\|_{\mathcal{L}_{2,i}} = \|\Psi_o^\dagger \Psi_o \Psi_c \Psi_c^\dagger\|_{\mathbb{R}^{n,i}} \\
&= \|\mathbf{W}_o \mathbf{W}_c\|_{\mathbb{R}^{n,i}} = \|\sqrt{\mathbf{W}_o \mathbf{W}_c}\|_{\mathbb{R}^{n,i}}^2 \\
&= \sigma_{\max}^2(\sqrt{\mathbf{W}_o \mathbf{W}_c}).
\end{aligned} \tag{15}$$

In fact, if the system is controllable and observable, the entire nonzero spectrum of $\Gamma_G^\dagger \Gamma_G$ can be obtained.

$$\begin{aligned}
&\text{nonzero squared singular values of } \Gamma_G = \text{nonzero eigenvalues of } \Gamma_G^\dagger \Gamma_G \\
&= \text{nonzero eigenvalues of } \Psi_c^\dagger \Psi_o^\dagger \Psi_o \Psi_c = \text{eigenvalues of } \Psi_o^\dagger \Psi_o \Psi_c \Psi_c^\dagger \\
&= \text{eigenvalues of } \mathbf{W}_o \mathbf{W}_c = \text{eigenvalues of } \mathbf{W}_c \mathbf{W}_o
\end{aligned} \tag{16}$$

The singular values of Γ_G are called the Hankel singular values (HSV). The nonzero HSV are the eigenvalues of $\sqrt{\mathbf{W}_c \mathbf{W}_o}$, the set of invariants mentioned at the end of the previous subsection.

The Hankel norm model reduction problem is useful for finding bounds for the full \mathcal{H}_∞ model reduction problem. In particular, it establishes the HSV as a measure of response.

Definition 2.3.2 (Hankel Norm Model Reduction Problem) Given a rank n Hankel operator Γ_G corresponding to a stable, causal, LTI system G , such that $\Gamma_G : \mathcal{L}_2^m[-T, 0] \rightarrow \mathcal{L}_2^p[0, T]$, find $\inf_{\text{rank}(\tilde{\Gamma}) \leq k} \|\Gamma_G - \tilde{\Gamma}\|_{\mathcal{L}_{2,i}}$ for $\tilde{\Gamma}$ a Hankel operator and $k < n$.

In order to motivate the solution to the above problem, we first need to introduce the following theorem.

Theorem 2.3.3 Given a rank n matrix $\mathbf{M} \in \mathbb{R}^{p \times r}$ ($n \leq \min(p, r)$) with nonzero singular values ordered such that $\sigma_1(\mathbf{M}) \geq \sigma_2(\mathbf{M}) \geq \dots \geq \sigma_n(\mathbf{M})$, for an arbitrary rank m matrix $\mathbf{S} \in \mathbb{R}^{p \times r}$ such that $m \leq k < n$,

$$\sigma_{\max}(\mathbf{M} - \mathbf{S}) \geq \sigma_{k+1}(\mathbf{M}) \tag{17}$$

Combining (13) and (15) and Theorem 2.3.3 leads to the next theorem. This is fundamental to this paper, for it solves the Hankel model reduction problem.

Theorem 2.3.4 Given a rank n Hankel operator Γ_G with nonzero singular values ordered such that $\sigma_1(\Gamma_G) \geq \sigma_2(\Gamma_G) \geq \dots \geq \sigma_n(\Gamma_G)$, for an arbitrary rank k Hankel operator $\tilde{\Gamma}$ such that $k < n$,

$$\|\Gamma_G - \tilde{\Gamma}\|_{\mathcal{L}_{2,i}} \geq \sigma_{k+1}(\Gamma_G) \tag{18}$$

A limitation of this theorem is that, for finite dimensional systems, there does not always exist a Hankel operator that makes the inequality an equality.

When equation (18) is combined with $\Gamma_G = P_+G|_{\mathcal{L}_2[-T,0]}$, we obtain a lower bound for G .

$$\begin{aligned} & \text{For order}(G) = n \text{ (i.e. McMillan Degree } n), \\ & \text{For all } \tilde{G} \text{ of order } k \leq r, \|G - \tilde{G}\|_{\mathcal{L}_2,i} \geq \sigma_{r+1}(\Gamma_G) \end{aligned} \quad (19)$$

An interpretation of this lower bound is that the best possible r^{th} -order approximation to the input-output behavior of the system is at least a “distance” $\sigma_{r+1}(\Gamma_G)$ away from the exact response. It implies that any reduced order model that projects out states corresponding to large singular values is necessarily a worse approximation than a model that projects out small singular values. Thus, states corresponding to large singular values contribute the most to the system’s response.

• **Balanced realizations**

It has been shown that the nonzero HSV correspond to the eigenvalues of $\sqrt{\mathbf{W}_c \mathbf{W}_o}$. This suggests that the Hankel operator is related to the system’s controllability and observability. This connection is important for many reasons. Firstly, interpreting the Hankel operator in terms of observability and controllability aids intuition. Secondly, the gramians’ eigenvalues are not invariant under coordinate transformations, so we still lack unambiguous measures of controllability and observability. Lastly, as we can see in Figure 2, controllability and observability may not be correlated. For generic realizations, observability and controllability are not on the same footing and consequently this leads to further ambiguity. Should model reduction be based on observability or controllability?

The resolution to these problems relies on determining the most suitable coordinates. This is equivalent to ascertaining the proper way to coarse grain the system. Our freedom in the choice of coordinates allows us to find a coordinate transformation, \mathbf{T} , such that, in the new coordinates, the controllability and observability gramians are equal and diagonal. The reader may note that this procedure is essentially the same as is used in filtering theory. This aligns the observability and controllability ellipsoids, thereby putting controllability and observability on the same footing. Furthermore, in these *balanced coordinates*, $\widetilde{\mathbf{W}}_c = \widetilde{\mathbf{W}}_o = \mathbf{\Sigma}$ where $\mathbf{\Sigma}$ is diagonal and has the same eigenvalues as $\sqrt{\mathbf{W}_c \mathbf{W}_o}$ (ordered from largest to smallest). The eigenvalues of the balanced gramians are the nonzero HSV, invariants of the system. The resulting system realization is known as a *balanced realization*.

\mathbf{T} can be constructed using the following algorithm [20]. By definition, there exists a coordinate transformation \mathbf{S} such that $\mathbf{S}^{-1} \mathbf{W}_c \mathbf{W}_o \mathbf{S} = \mathbf{\Sigma}^2$. Now supposing that $\mathbf{S} = \mathbf{W}_o^{-1/2} \mathbf{R}$ for some \mathbf{R} , $\mathbf{R}^{-1} \mathbf{W}_o^{1/2} \mathbf{W}_c \mathbf{W}_o^{1/2} \mathbf{R} = \mathbf{\Sigma}^2$.

Hence, $\mathbf{W}_o^{1/2}\mathbf{W}_c\mathbf{W}_o^{1/2}$ is Hermitian and similar to $\mathbf{\Sigma}^2$. Provided $\mathbf{\Sigma}$ does not have degenerate eigenvalues, there exists a unique unitary matrix \mathbf{U} such that $\mathbf{U}^\dagger\mathbf{W}_o^{1/2}\mathbf{W}_c\mathbf{W}_o^{1/2}\mathbf{U} = \mathbf{\Sigma}^2$. This means that

$$(\mathbf{\Sigma}^{-1/2}\mathbf{U}^\dagger\mathbf{W}_o^{1/2})\mathbf{W}_c(\mathbf{\Sigma}^{-1/2}\mathbf{U}^\dagger\mathbf{W}_o^{1/2})^\dagger = \mathbf{\Sigma}.$$

Thus, remembering that \mathbf{W}_c transforms as $\mathbf{W}_c \xrightarrow{\mathbf{T}} \widetilde{\mathbf{W}}_c = \mathbf{T}^{-1}\mathbf{W}_c(\mathbf{T}^\dagger)^{-1}$, if we let $\mathbf{T}^{-1} = \mathbf{\Sigma}^{-1/2}\mathbf{U}^\dagger\mathbf{W}_o^{1/2}$, we have found the desired coordinate transformation. It follows that:

$$\begin{aligned} \mathbf{T}^\dagger\mathbf{W}_o\mathbf{T} &= (\mathbf{\Sigma}^{1/2}\mathbf{U}^\dagger\mathbf{W}_o^{-1/2})\mathbf{W}_o(\mathbf{W}_o^{-1/2}\mathbf{U}\mathbf{\Sigma}^{1/2}) \\ &= \mathbf{\Sigma}^{1/2}\mathbf{U}^\dagger\mathbf{U}\mathbf{\Sigma}^{1/2} = \mathbf{\Sigma}. \end{aligned} \quad (20)$$

In general, if a system is not controllable and observable, such a \mathbf{T} (balancing transformation) does not exist. It is possible to find a balancing transformation such that:

$$\mathbf{W}_c = \begin{bmatrix} \mathbf{\Sigma} & 0 & 0 & 0 \\ 0 & \mathbf{\Sigma}_1 & 0 & 0 \\ 0 & 0 & 0 & 0 \\ 0 & 0 & 0 & 0 \end{bmatrix} \text{ and } \mathbf{W}_o = \begin{bmatrix} \mathbf{\Sigma} & 0 & 0 & 0 \\ 0 & 0 & 0 & 0 \\ 0 & 0 & \mathbf{\Sigma}_2 & 0 \\ 0 & 0 & 0 & 0 \end{bmatrix}, \quad (21)$$

where $\mathbf{\Sigma}$, $\mathbf{\Sigma}_1$, and $\mathbf{\Sigma}_2$ are all diagonal. $\mathbf{\Sigma}$ is the matrix of HSV and the corresponding subsystem is controllable and observable. The subsystem associated with $\mathbf{\Sigma}_1$ is controllable and unobservable, while the one associated with $\mathbf{\Sigma}_2$ is uncontrollable and observable.

- **Balanced truncation**

Now we possess the tools to generate reduced-order models. The reduction technique in what follows is called *balanced truncation*. We assume that the system is stable, controllable and observable, and has been transformed into a balanced realization. Additionally, since the system is stable, we consider the problem over an infinite time horizon (i.e. $T \rightarrow \infty$).

Given a system satisfying the above assumptions, decompose the matrix of ordered HSV $\mathbf{\Sigma}$ (ordered from largest to smallest) such that the first r eigenvalues form the matrix $\mathbf{\Sigma}_L$. The remainder form the matrix of smaller singular values $\mathbf{\Sigma}_S$. Decompose $\mathbf{\Sigma}_L$ and $\mathbf{\Sigma}_S$ such that they have no common eigenvalues. The realization for the full system takes the form:

$$\begin{aligned} \tilde{\mathbf{A}} &= \begin{bmatrix} \tilde{\mathbf{A}}_L & \tilde{\mathbf{A}}_{12} \\ \tilde{\mathbf{A}}_{21} & \tilde{\mathbf{A}}_S \end{bmatrix}, \quad \tilde{\mathbf{B}} = \begin{bmatrix} \tilde{\mathbf{B}}_L \\ \tilde{\mathbf{B}}_S \end{bmatrix}, \\ \tilde{\mathbf{C}} &= \begin{bmatrix} \tilde{\mathbf{C}}_L & \tilde{\mathbf{C}}_S \end{bmatrix}. \end{aligned} \quad (22)$$

By projecting out the states corresponding to $\mathbf{\Sigma}_S$, the remaining three matrices, $(\tilde{\mathbf{A}}_L, \tilde{\mathbf{B}}_L, \tilde{\mathbf{C}}_L)$, form an r -dimensional realization that approximates

the original system. Denote the input-output operator for the reduced system by \tilde{G}_r . This realization, by construction, is stable and balanced. Its HSV are the eigenvalues of Σ_L . In addition, the approximation error is given by:

$$\|G - \tilde{G}_r\|_{\mathcal{L}_2, i} \leq 2 \sum_{j=1}^k \sigma_{i_j}^{\text{dist}}, \quad (23)$$

where $\{\sigma_{i_j}^{\text{dist}} : 1 \leq j \leq k\}$ is the distinct HSV in Σ_S .

These techniques are extended to unstable systems in Appendix A. This makes it possible to use these techniques on linear, conservative systems. A particularly relevant result is:

Theorem 2.3.5 (Lower Bound) Given a LTI, causal system G with n dimensional minimal realization $(\mathbf{A}, \mathbf{B}, \mathbf{C})$. If there exists an “ a ” such that $-a\mathbf{I} + \mathbf{A}$ is a stable system matrix then for any order r (or less) approximant \tilde{G}_r

$$\|G - \tilde{G}_r\|_{\mathcal{L}_2[0, T], i} \geq (1 - e^{-2aT} \|e^{\mathbf{A}^\dagger T} e^{\mathbf{A} T}\|_{\mathbb{C}^n, i}) \sigma_{r+1}(a)$$

It is the subject of the next section to apply these methods to general oscillator systems, whereupon, when combined with the spatial content of the reductions, specifies how to coarse grain.

3 Reduction of Oscillator Systems

The standard form for the equations of motion generated by a quadratic Hamiltonian with $2N$ phase space degrees of freedom is given by

$$\begin{bmatrix} \dot{q} \\ \dot{p} \end{bmatrix} = \begin{bmatrix} 0 & \mathbf{\Omega} \\ -\mathbf{\Omega} & 0 \end{bmatrix} \begin{bmatrix} q \\ p \end{bmatrix}, \quad (24)$$

where $\mathbf{\Omega}$ is a $N \times N$ positive definite matrix. These systems are typically associated with coupled harmonic oscillators. Furthermore, these systems are considered trivial because when expressed in normal modes, the resulting oscillators are decoupled. Decoupled oscillators are considered noninteracting. This view is correct for isolated systems, however, for open systems it is not.

The coordinates that capture the original experimental configuration is of exceptional interest. This is because the important coordinate system for model reduction is the one in which the gramians are balanced. Now while in balanced coordinates the gramians are diagonalized, the matrices \mathbf{A} or $\mathbf{\Omega}$ need not be. This illustrates that a generic open system, even a linear one, typically has interacting internal states. The statistical mechanics of quadratic Hamiltonians is invalid unless the system is driven. This follows

since when expressed in normal modes, the system is noninteracting and, hence, not ergodic or mixing [13, 14]. The usual heuristic argument for justifying the practice is that phonon (oscillator) systems do not truly have a linear dispersion; the systems themselves are nonlinear. The nonlinearity is responsible for the mixing of states. This is precisely the issue that spawned the Fermi-Pasta-Ulam (FPU) problem ¹⁰. Once the nonlinearity from the heuristic argument is associated to a disturbance of the form $\mathbf{B}u(t)$, then the analysis in this paper agrees with the heuristic argument.

The advantages of using balanced coordinates rather than modal coordinates reflect the sensitivity of the system to the choice of experiment. This sensitivity to experiment suggests that it is more appropriate for oscillator systems ¹¹ to investigate open systems.

$$\dot{z} = \begin{bmatrix} \dot{z}_1 \\ \dot{z}_2 \end{bmatrix} = \mathbf{A}z + \mathbf{B}u = \begin{bmatrix} 0 & \mathbf{I} \\ -\Omega^2 & 0 \end{bmatrix} \begin{bmatrix} z_1 \\ z_2 \end{bmatrix} + \mathbf{B}u \quad (25)$$

$$y = \mathbf{C}z$$

In this coordinate system, z_1 represents the spring displacements while z_2 represents the corresponding velocities.

There remains the question of which experiments should be considered. Conceptually, \mathbf{B} varies the gains of the driving. \mathbf{B} determines how accessible particular states are to driving. Alternatively, allowing for Dirac delta driving and setting $z_0 = 0$, the driving may be used to prepare the system's initial conditions. With this interpretation, \mathbf{B} prescribes how initial conditions are weighted. Similarly, \mathbf{C} indicates which and how easily internal states are measured. We exclusively consider oscillator systems with uniform constituent sizes and masses. This choice, motivated by thermodynamics and the equipartition of energy, implies that positions and momenta are treated equally. This is equivalent to assuming that the position and momentum of each particle can be driven with equal gain. Hence, $\mathbf{B} = b\mathbf{I}$, where b is a constant. Considering each position and momentum equally difficult to measure corresponds to setting $\mathbf{C} = c\mathbf{I}$. Now let $b = c = 1$. Mathematically this choice is natural since the resulting input-output operator (in the Laplace domain) is the full system's resolvent, $(s\mathbf{I} - \mathbf{A})^{-1}$.

Fixing \mathbf{B} and \mathbf{C} dictates the type of experiment. However, it does not fully determine the experiment. For the problem to be well-posed, we also need to specify the duration of the experiment. This is important because the exact form of the experiment fully determines its input-output characteristics (i.e. the input-output operator). Different experiments give rise

¹⁰It is interesting to note that coupled, nonlinear, anharmonic oscillator systems are not guaranteed to mix. This fact has been attributed to the existence soliton solutions to the equations of motions.

¹¹At least oscillator systems with uniform masses.

to different measures of response. This is illustrated in Figure 3. As a reminder, Hankel singular values (HSV) tell us how much their corresponding states contribute to the response. These states are roughly the system’s input-output resonances.

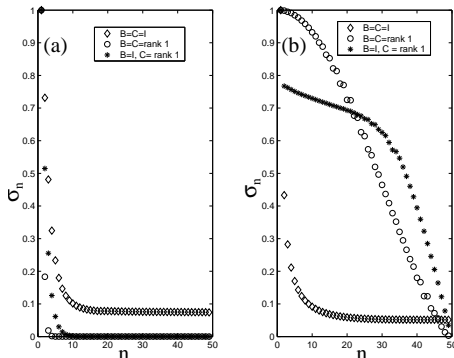


Figure 3: A plot of the ordered Hankel singular values (HSV) for the homogeneous, harmonic oscillator chain. T is the time over which the system is investigated. The HSV in (a) are plotted for $T \propto N^{1/2}$, while $T \propto N^2$ for (b), where N is the total number of masses in the chain. In each case $N = 49$.

Figure 3(b) depicts how different types of experiments on an oscillator system, over the same duration, $T = N^2$, give rise to different normalized HSV and, consequently, different measures of response. Figure 3(a) displays the same types of experiments, but with $T = N^{1/2}$. Clearly, the normalized HSV for two of the experiments have completely changed. Figure 3(a) demonstrates that experiments over the shorter time frames tend to admit lower-order reduced models. Hence, time scales have an enormous impact on model reduction.

Although experiments over short time horizons directly lead to very low-order reduced models [2], our intent for introducing a finite cutoff time is to regulate divergences. The divergences arise due to the fact that the HSV become infinite in the infinite-time horizon limit. This is discussed in more detail in Appendix A. Now with the divergences regulated, we return to addressing how to coarse grain physical systems. From above, we learn that this is not a well-posed question since different time scales or experiments lead to different reductions. A well-posed reduction problem requires specifying the type of experiment and the time scale. It is natural to expect that past a certain time scale (i.e. past thermodynamic equilibration), there is a unique way to coarse grain. It is for this reason that we approximate the response of the system in equation (25) with $\mathbf{B} = \mathbf{C} = \mathbf{I}$ over a finite yet long time horizon. Interestingly, not only does there exist such a time scale, but some Hankel norm results determine precisely the

coarse grainings. These topics comprise the following subsections, the first in which we work without restriction on the form of $\mathbf{\Omega}$ other than that it is positive definite. In the second subsection we consider the case of the homogeneous linear harmonic chain, and lastly we treat some heterogeneous linear oscillator chains.

3.1 General Oscillator Systems

To determine the best possible coarse graining or at least near the optimal coarse graining, we will proceed to use the Hankel operator machinery to obtain bounds for $\|G - \tilde{G}_r\|_{\mathcal{L}_2[0,T],i}$. Recalling the control theory tutorial, this provides us with a criterion for model reduction. In particular, the lower bound,

$$\|G - \tilde{G}\|_{\mathcal{L}_2,i} \geq \sigma_{r+1}(\Gamma_G),$$

where $\sigma_{r+1}(\Gamma_G)$ is the $(r+1)^{\text{th}}$ HSV, confirms that the states with large HSV contribute the most to the response. The upper bound,

$$\|G - \tilde{G}\|_{\mathcal{L}_2,i} \leq 2 \sum_{j=1}^k \sigma_{i_j}^{\text{dist}},$$

where $\{\sigma_{i_j}^{\text{dist}} : 1 \leq j \leq k\}$ is the set of distinct HSV with $i_j > r$, ensures that our approximations are controlled. The first step is to determine the HSV that provide these bounds. However, in doing so we also find the balancing transformation. This makes it trivial to truncate the system and obtain reduced-order models.

Determining the HSV requires calculating the controllability and observability gramians. Unfortunately, restricting attention to a finite cutoff time complicates the analysis. For instance, \mathbf{W}_c and \mathbf{W}_o satisfy differential equations (see equations (10) and (11)) instead of Lyapunov equations. A method of simplifying the analysis involves investigating the system matrix $-a\mathbf{I} + \mathbf{A}$ over an infinite time horizon instead of \mathbf{A} over a finite time horizon. This procedure is known as exponential discounting. Intuitively “ a ” should be on the order of the inverse time cutoff for the approximation to be any good. Fortunately the above intuition can be made much more rigorous, thereby keeping all approximations under control.

For the systems under consideration, the gramians are formally given by

$$\begin{aligned} \mathbf{W}_c &= \int_0^T e^{\mathbf{A}t} e^{\mathbf{A}^\dagger t} dt \Rightarrow \mathbf{W}_c^{(a)} = \int_0^\infty e^{-2at} e^{\mathbf{A}t} e^{\mathbf{A}^\dagger t} dt, \\ \mathbf{W}_o &= \int_0^T e^{\mathbf{A}^\dagger t} e^{\mathbf{A}t} dt \Rightarrow \mathbf{W}_o^{(a)} = \int_0^\infty e^{-2at} e^{\mathbf{A}^\dagger t} e^{\mathbf{A}t} dt. \end{aligned} \quad (26)$$

A property of these gramians is that $\mathbf{W}_c \mathbf{W}_o$ or $\mathbf{W}_c^{(a)} \mathbf{W}_o^{(a)}$ are always similar to a matrix of the form $\begin{bmatrix} \mathbf{M} & 0 \\ 0 & \mathbf{M}^\dagger \end{bmatrix}$. This means that there is

an exact duplicity in the HSV independent of “ a ”. In fact, under the transformation \mathbf{R} defined in Appendix B, \mathbf{A} takes the form of the system matrix in equation (24). In this basis, we find that $\widetilde{\mathbf{W}}_c \approx \widetilde{\mathbf{W}}_o$ where

$$\begin{aligned} \widetilde{\mathbf{W}}_c = \frac{1}{4a} & \begin{bmatrix} \boldsymbol{\Omega} + \boldsymbol{\Omega}^{-1} + \mathcal{O}(a^2) & 0 \\ 0 & \boldsymbol{\Omega} + \boldsymbol{\Omega}^{-1} + \mathcal{O}(a^2) \end{bmatrix} \\ & + \frac{1}{4} \begin{bmatrix} 0 & \boldsymbol{\Omega}^{-2} - \mathbf{I} + \mathcal{O}(a^2) \\ \boldsymbol{\Omega}^{-2} - \mathbf{I} + \mathcal{O}(a^2) & 0 \end{bmatrix}. \end{aligned} \quad (27)$$

In this basis the gramians are almost balanced. Provided we transform the system by a unitary transformation, \mathbf{U}_d , to diagonalize $\boldsymbol{\Omega}$ (i.e. $\boldsymbol{\Omega} \xrightarrow{\mathbf{U}_d} \boldsymbol{\Lambda}_\Omega$) and we take “ a ” sufficiently small (sufficiently long-time horizons), the gramians are balanced. The precise interpretation of “sufficiently small” is outlined in Appendix C. We want to require that “ a ” is small enough so that the off-diagonal terms do not change the ordering of the HSV. Here we assume, without loss of generality, that the eigenvalues of $\boldsymbol{\Lambda}_\Omega$ are ordered from smallest to largest. Under the previously mentioned conditions to $\mathcal{O}(a^2)$ the balanced gramians (balanced up to permutation) take the form

$$\bar{\mathbf{W}}_c = \bar{\mathbf{W}}_o = \frac{1}{4a} \begin{bmatrix} \boldsymbol{\Lambda}_\Omega + \boldsymbol{\Lambda}_\Omega^{-1} + \mathcal{O}(a^2) & \mathcal{O}(a) \\ \mathcal{O}(a) & \boldsymbol{\Lambda}_\Omega + \boldsymbol{\Lambda}_\Omega^{-1} + \mathcal{O}(a^2) \end{bmatrix}. \quad (28)$$

These balanced gramians are associated with the linear system

$$\begin{aligned} \begin{bmatrix} \dot{\bar{z}}_1 \\ \dot{\bar{z}}_2 \end{bmatrix} &= \begin{bmatrix} 0 & \boldsymbol{\Lambda}_\Omega \\ -\boldsymbol{\Lambda}_\Omega & 0 \end{bmatrix} \begin{bmatrix} \bar{z}_1 \\ \bar{z}_2 \end{bmatrix} + \begin{bmatrix} \boldsymbol{\Lambda}_\Omega^{1/2} \mathbf{U}_d^\dagger & 0 \\ 0 & \boldsymbol{\Lambda}_\Omega^{-1/2} \mathbf{U}_d^\dagger \end{bmatrix} \begin{bmatrix} u_1 \\ u_2 \end{bmatrix}, \\ \begin{bmatrix} y_1 \\ y_2 \end{bmatrix} &= \begin{bmatrix} \mathbf{U}_d \boldsymbol{\Lambda}_\Omega^{-1/2} & 0 \\ 0 & \mathbf{U}_d \boldsymbol{\Lambda}_\Omega^{1/2} \end{bmatrix} \begin{bmatrix} \bar{z}_1 \\ \bar{z}_2 \end{bmatrix}. \end{aligned} \quad (29)$$

Given that $\lambda_j(\boldsymbol{\Omega}) \leq \lambda_k(\boldsymbol{\Omega})$ for all $j < k$, let α be a permutation such that $\lambda_{\alpha(j)}(\boldsymbol{\Omega}) + \lambda_{\alpha(j)}^{-1}(\boldsymbol{\Omega}) \leq \lambda_{\alpha(k)}(\boldsymbol{\Omega}) + \lambda_{\alpha(k)}^{-1}(\boldsymbol{\Omega})$ for all $k < j$. Trivially, via a unitary transformation, the gramians in equation (28) may be fully balanced (the HSV are ordered). In this case, we find that

$$\sigma_k(a) = \frac{1}{4a} (\lambda_{\lceil \frac{\alpha(k)}{2} \rceil}(\boldsymbol{\Omega}) + \lambda_{\lceil \frac{\alpha(k)}{2} \rceil}^{-1}(\boldsymbol{\Omega})) + \mathcal{O}(1). \quad (30)$$

The degeneracy of the HSV suggests that any balanced truncation that keeps states corresponding to the first $r = 2q$ HSV will remain conservative. In fact, we can see this by inspection of equation (29). With this in mind, we will consider only truncations that keep an even number of states. The immediate consequences of these results are that we obtain bounds on the approximation error of the response.

$$\begin{aligned} \|G - \tilde{G}_{2q}\|_{\mathcal{L}_2[0,T],i} &\geq (1 - e^{-2aT}) \sigma_{2q+1}(a) \\ &= \frac{1}{4a} (1 - e^{-2aT}) (\lambda_{\alpha(q+1)}(\boldsymbol{\Omega}) + \lambda_{\alpha(q+1)}^{-1}(\boldsymbol{\Omega})), \end{aligned} \quad (31)$$

and

$$\begin{aligned} \|G - \tilde{G}_{2q}\|_{\mathcal{L}_2[0,T],i} &\leq 2e^{aT} \sum_{j=q}^{N-1} \sigma_{2j+1}(a) \\ &= \frac{1}{2a} e^{aT} \sum_{j=q+1}^N \lambda_{\alpha(j)}(\mathbf{\Omega}) + \lambda_{\alpha(j)}^{-1}(\mathbf{\Omega}). \end{aligned} \quad (32)$$

Additionally, by using linear-matrix-inequality (LMI) techniques [26], a substantially tighter upper bound can be established. The improved bound is

$$\begin{aligned} \|G - \tilde{G}_{2q}\|_{\mathcal{L}_2[0,T],i} &\leq 2e^{aT} \sigma_{2k+1}(a) \\ &= \frac{1}{2a} e^{aT} (\lambda_{\alpha(k+1)}(\mathbf{\Omega}) + \lambda_{\alpha(k+1)}^{-1}(\mathbf{\Omega})). \end{aligned} \quad (33)$$

A remarkable aspect of these oscillator models is that, over a long time horizon, the relation between the system's spectrum and the gramians is simple. Despite this simple relationship, these results also establish that the set of best reductions (i.e. those that satisfy the lower bound) need not be modal reductions! Modal reductions explicitly neglect (project out) the system's fast dynamics. For instance, let us suppose that $\lambda_j(\mathbf{\Omega}) \geq 1$ for all j ; disregarding degeneracy, the HSV are automatically ordered from smallest to largest. This implies that projecting out small HSV eliminates states corresponding to slow modes! This is contrary to what is typically done. Alternatively, suppose that $\lambda_j(\mathbf{\Omega}) < 1$ for all j . In this instance, disregarding degeneracy, the HSV are ordered from largest to smallest. This is precisely when modal reduction is appropriate. Lastly, when the eigenvalues of $\mathbf{\Omega}$ are both greater than and less than one, the appropriate reductions involve a mixing of fast and slow modes.

In the basis that produces the realization in equation (29), the system is balanced, and yet $\mathbf{\Omega}$ is diagonalized. Although this means that such systems are noninteracting, not all internal states are treated equally. In fact, in the case of the linear harmonic chain, the weighting of the gains has a physically meaningful interpretation that will be elaborated upon in Section 3.2. Also, there is an enormous degeneracy in the types of experiments producing equivalent reductions. The same reductions result from using $\mathbf{B} = \mathbf{V}$ and $\mathbf{C} = \mathbf{U}$ where \mathbf{V} and \mathbf{U} are arbitrary unitary matrices. This may not come as much of a surprise since requiring \mathbf{V} and \mathbf{U} to be unitary causes the internal states to be treated equally. We see that there are an infinite number of inequivalent realizations that yield the same reduction.

These results also reveal how to choose “ a ”. By varying “ a ” we may refine our bounds. Generally, we have an LTI, causal system that achieves or almost achieves the lower bound. Consequently, it is useful to choose “ a ” such that the lower bound is at its maximum. The maximum occurs

as $a \rightarrow 0$.

$$\|G - \tilde{G}_{2q}\|_{\mathcal{L}_2[0,T],i} \geq \frac{T}{2}(\lambda_{\alpha(q+1)}(\mathbf{\Omega}) + \lambda_{\alpha(q+1)}^{-1}(\mathbf{\Omega})) \quad (34)$$

For the lowest upper bound (from balanced truncation), $\frac{d}{da}[2e^{aT}\sigma_{2k+1}(a)] = 0$ implies that $a = T^{-1}$. Therefore, the minimum upper bound is

$$\|G - \tilde{G}_{2q}\|_{\mathcal{L}_2[0,T],i} \leq \frac{eT}{2}(\lambda_{\alpha(q+1)}(\mathbf{\Omega}) + \lambda_{\alpha(q+1)}^{-1}(\mathbf{\Omega})). \quad (35)$$

As we approximate G over an infinite-time horizon ($T \rightarrow \infty$), both the norm of G and the absolute error diverge. This divergence is unavoidable and generally independent of the number of particles (oscillators) in the system. However, there is another possible interpretation if the number of particles, N , is large. For our analytics to be valid, there must be restrictions on the size of “ a ”. Combining equations (71) and (73) from Appendix C, we are able to relate the maximal “ a ” to the frequencies of the system, $\lambda_k(\mathbf{\Omega})$. In most cases, as N gets large, $\lambda_k(\mathbf{\Omega}) \sim N^{-\delta_1}$. For instance, in the case of the homogeneous linear harmonic chain, for small wave number, $\delta_1 = 1$. Consequently, “ a ” is forced to fall to zero asymptotically like $a \sim N^{-\delta_2}$ for some $\delta_2 > 0$ as $N \rightarrow \infty$. Reciprocally, if “ a ” tends to zero faster and, consequently, T tends to infinity, there is no restriction on N . The divergence is due to the infinite time horizon. Suppose that “ a ” is parameterized by N and we consider the $N \rightarrow \infty$ limit. In this case, the divergence is due to the infinite-particle limit. For oscillator systems, like photons and phonons, the divergence is attributable to the absence of a mass gap (i.e. the eigenvalues of $\mathbf{\Omega}$ become dense near zero). Thus, there is no inherent length (mass) scale for the system. This is one of the simplest divergences, a long wavelength divergence. Depending on the structure of $\mathbf{\Lambda}_{\Omega}$, however, there may also be a short-wavelength divergence or even possibly a mixed-wavelength divergence. Had we investigated yet a shorter time scale, still taking $T \rightarrow \infty$, the resulting reduced-order systems are typically dissipative [3, 2]. Physically this is a manifestation of how fluctuations may induce time scales [13, 14].

While the divergence in $\|G\|_{\mathcal{L}_2,i}$ and $\|G - \tilde{G}_r\|_{\mathcal{L}_2,i}$ has been explained, its consequences have not. Since the error estimate diverges, except when regulated (i.e. by considering finite T), the absolute error is not a meaningful quantity. Any long-time approximate is asymptotic at best. This means that the (regulated) relative error, $\lim_{T \rightarrow \infty} \|G - \tilde{G}_r\|_{\mathcal{L}_2[0,T],i} / \|G\|_{\mathcal{L}_2[0,T],i}$, is much more useful. Combining equations (31) and (32) yield rather con-

servative bounds:

$$\begin{aligned} \lim_{T \rightarrow \infty} \frac{\|G - \tilde{G}_{2q}\|_{\mathcal{L}_2[0,T],i}}{\|G\|_{\mathcal{L}_2[0,T],i}} &\geq \lim_{T \rightarrow \infty} \frac{\frac{T}{2}(\lambda_{\alpha(q+1)}(\mathbf{\Omega}) + \lambda_{\alpha(q+1)}^{-1}(\mathbf{\Omega}))}{\frac{eT}{2} \sum_{j=1}^N \lambda_{\alpha(j)}(\mathbf{\Omega}) + \lambda_{\alpha(j)}^{-1}(\mathbf{\Omega})} \\ &= \frac{\lambda_{\alpha(q+1)}(\mathbf{\Omega}) + \lambda_{\alpha(q+1)}^{-1}(\mathbf{\Omega})}{e \text{Tr}(\mathbf{\Omega} + \mathbf{\Omega}^{-1})}, \end{aligned} \quad (36)$$

and

$$\begin{aligned} \lim_{T \rightarrow \infty} \frac{\|G - \tilde{G}_{2q}\|_{\mathcal{L}_2[0,T],i}}{\|G\|_{\mathcal{L}_2[0,T],i}} &\leq \lim_{T \rightarrow \infty} \frac{\frac{eT}{2} \sum_{j=q+1}^N \lambda_{\alpha(j)}(\mathbf{\Omega}) + \lambda_{\alpha(j)}^{-1}(\mathbf{\Omega})}{\frac{T}{2}(\lambda_{\alpha(1)}(\mathbf{\Omega}) + \lambda_{\alpha(1)}^{-1}(\mathbf{\Omega}))} \\ &= \frac{e \sum_{j=q+1}^N \lambda_{\alpha(j)}(\mathbf{\Omega}) + \lambda_{\alpha(j)}^{-1}(\mathbf{\Omega})}{(\lambda_{\alpha(1)}(\mathbf{\Omega}) + \lambda_{\alpha(1)}^{-1}(\mathbf{\Omega}))}. \end{aligned} \quad (37)$$

Comparatively tighter bounds are obtained by using equations (34) and (35). These bounds are

$$\lim_{T \rightarrow \infty} \frac{\|G - \tilde{G}_{2q}\|_{\mathcal{L}_2[0,T],i}}{\|G\|_{\mathcal{L}_2[0,T],i}} \geq \frac{\lambda_{\alpha(q+1)}(\mathbf{\Omega}) + \lambda_{\alpha(q+1)}^{-1}(\mathbf{\Omega})}{e(\lambda_{\alpha(1)}(\mathbf{\Omega}) + \lambda_{\alpha(1)}^{-1}(\mathbf{\Omega}))}, \quad (38)$$

and

$$\lim_{T \rightarrow \infty} \frac{\|G - \tilde{G}_{2q}\|_{\mathcal{L}_2[0,T],i}}{\|G\|_{\mathcal{L}_2[0,T],i}} \leq \frac{e(\lambda_{\alpha(q+1)}(\mathbf{\Omega}) + \lambda_{\alpha(q+1)}^{-1}(\mathbf{\Omega}))}{\lambda_{\alpha(1)}(\mathbf{\Omega}) + \lambda_{\alpha(1)}^{-1}(\mathbf{\Omega})}. \quad (39)$$

These general cases have allowed us, for instance, to determine conditions when modal reduction is appropriate. Without knowing more about $\mathbf{\Omega}$ it is not possible to discern the spatial content of the reductions. Without the spatial content we cannot specify the relationship between reduction type and coarse graining. In the following section, we will apply the above results to the linear harmonic chain, from which we determine the appropriate coarse grainings. This example will clarify the relationship between system reductions and coarse grainings.

3.2 The Linear Harmonic Chain

The models that we consider in this section are all variants of the one-dimensional linear harmonic chain depicted in Figure 4. The system consists of a chain of N equally spaced masses each with mass m connected via $N + 1$ springs. The chain is connected on each side to stationary walls. We will first treat coarse graining the linear harmonic chain with homogeneous springs in great detail. Briefly, we also present how to coarse grain some heterogeneous chains. We will conclude by comparing the different models and their respective coarse grainings.

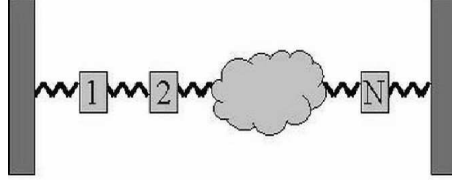


Figure 4: Linear chain of oscillators with fixed boundary conditions. All of our models are of this form. The different variations have homogeneous, layered, and randomly, uniformly sampled spring constants.

• **The homogeneous chain**

Each spring of the homogeneous linear chain has a spring constant, k . For this system, Ω^2 has the familiar form,

$$\Omega^2 = \frac{k}{m} \begin{bmatrix} 2 & -1 & 0 & \dots & 0 \\ -1 & \ddots & \ddots & \ddots & \vdots \\ 0 & \ddots & \ddots & \ddots & 0 \\ \vdots & \ddots & \ddots & \ddots & -1 \\ 0 & \dots & 0 & -1 & 2 \end{bmatrix} \quad (40)$$

The matrix of ordered eigenvalues of Ω , Λ_Ω , is such that $(\Lambda_\Omega)_{pp} = \omega_p = 2\sqrt{\frac{k}{m}} \sin\left(\frac{\pi p}{2(N+1)}\right)$. Additionally, the unitary matrix that diagonalizes

Ω , \mathbf{U}_d , is given by $(\mathbf{U}_d)_{ij} = (\mathbf{u}^{(j)})_i = \sqrt{\frac{2}{N+1}} \sin\left(\frac{\pi ij}{N+1}\right)$. Here $\mathbf{u}^{(j)}$ is the eigenvector such that $\Omega \mathbf{u}^{(j)} = \omega_j \mathbf{u}^{(j)}$. Not only is \mathbf{U}_d both orthogonal and symmetric; its action on vectors is almost that of a discrete Fourier transform. It is not actually a Fourier transform since the spatial domain of lattice sites is not translationally invariant. Had we considered the linear harmonic chain on a ring instead (i.e. the group \mathbb{Z}_N), then the action of \mathbf{U}_d on vectors would, in fact, be a Fourier transform. The main point here is that local spatial rescaling in real space corresponds to rescaling large wave vectors in Fourier space.

Motivated by model reduction, we consider two particularly interesting limits. For the first case, let $2\sqrt{\frac{k}{m}} \leq 1$ and $N \gg 1$. In the second case we take the mass and spring constants to be functions of N such that $2\sqrt{\frac{k(N)}{m(N)}} \geq \frac{2(N+1)}{\pi}$ and $N \gg 1$. The former case will be discussed in detail. After that the nuances of latter case will be clear.

In the first case, $\omega_p < 1$ for all $p \in \{1, \dots, N\}$. Consequently, $\alpha(p) = p$. Hence, the HSV are already ordered from largest to smallest. Also, the

minimal time scale over which this analysis is valid is determined by the limits on “ a ”. When “ a ” satisfies the inequality in equation (73), which implies “ a ” at least scales as N^{-2} (if not faster in N), the ordering of the HSV is not altered. This gives the absolute error bounds when combined with the expression for ω_p and equations (34) and (35).

$$\begin{aligned} \|G - \tilde{G}_{2q}\|_{\mathcal{L}_2[0,T],i} &\geq \frac{T}{2} \left(\sin\left(\frac{\pi(q+1)}{2(N+1)}\right) + \left(\sin\left(\frac{\pi(q+1)}{2(N+1)}\right)\right)^{-1} \right) \\ &= \frac{NT}{\pi(q+1)} \left(1 + \mathcal{O}\left(\left(\frac{q+1}{N}\right)^2\right) \right) \end{aligned} \quad (41)$$

$$\begin{aligned} \|G - \tilde{G}_{2q}\|_{\mathcal{L}_2[0,T],i} &\leq \frac{\epsilon T}{2} \left(\sin\left(\frac{\pi(q+1)}{2(N+1)}\right) + \left(\sin\left(\frac{\pi(q+1)}{2(N+1)}\right)\right)^{-1} \right) \\ &= \frac{\epsilon NT}{\pi(q+1)} \left(1 + \mathcal{O}\left(\left(\frac{q+1}{N}\right)^2\right) \right) \end{aligned} \quad (42)$$

It is no surprise that the appropriate reductions project out the fast modes since in this limit the dispersion is linear. In the limit of large N , truncating fast modes is the same as projecting out large wave numbers. However, as mentioned earlier, large wave numbers correspond to short distances. So we see that projecting out fast modes from this system is equivalent to locally coarse graining. In fact, the lower bound suggests a stronger result. Provided the lower bound is approximately achievable, though the reduced-order system may not be LTI, the *best possible* reductions must involve locally coarse graining (modally reducing) the system. For example, projecting out a slow mode via balanced truncation is an example of nonlocal coarse graining. The lower bound of the incurred approximation error involves the HSV corresponding to that nonlocal state. Since the HSV corresponding to slow (nonlocal) modes are larger than those of fast modes, any nonlocal approximant of the system is necessarily worse by equation (41).

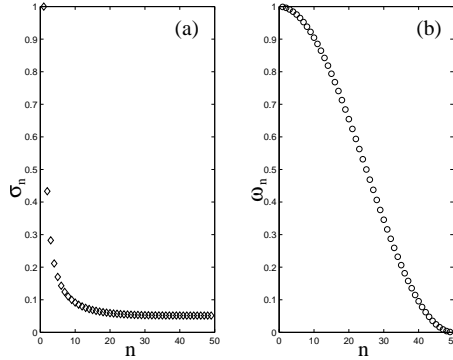


Figure 5: (a) A plot of the ordered Hankel singular values (HSV) for the homogeneous, harmonic oscillator chain. The spring constants are uniformly

taken to be $k = 0.25$. The HSV are plotted for $T \propto N^2$ where $N = 49$. The distribution of HSV remains essentially unchanged for any larger choice of T . (b) A plot of the frequencies for the same system.

The bounds in equations (41) and (42) also, at least for this model, provide information regarding finite size effects. If we take the lattice spacing to be b and the system size of the approximate system to be $L = qb$, the bounds then imply that (for $N \gg 1$)

$$\lim_{T \rightarrow \infty} \frac{\|G - \tilde{G}_{2q}\|_{\mathcal{L}_2[0,T],i}}{\|G\|_{\mathcal{L}_2[0,T],i}} = \mathcal{O}(L^{-1}). \quad (43)$$

This result is not new, though these techniques provide a new way to obtain it. Additionally, these techniques imply that for more general systems or experiments, reductions may have quite a different dependence on the system size.

It is apparent from (29) that the balanced realization for the harmonic chain weights driving of the momenta by $\Lambda_\Omega^{-1/2} \mathbf{U}_d$. Since $(\Lambda_\Omega)_{pp} = \omega_p \xrightarrow{N \gg 1} \frac{\pi p}{2N}$, this gives more weight to momenta corresponding to small frequencies. Therefore it requires smaller gains to activate the slower modes. If driving gives nontrivial initial conditions (i.e. impulses), this is equivalent to slow-mode initial conditions being more easily excited than fast-mode initial conditions. While the balanced realization of the system implies that the internal states of the system are noninteracting, it also implies that differing normal modes are not treated equally. This again suggests that the most natural coarse grainings are local coarse grainings.

Consider the latter conditions mentioned earlier, $2\sqrt{\frac{k(N)}{m(N)}} \geq \frac{2(N+1)}{\pi}$ and $N \gg 1$. Here $\omega_p > 1$ for all $p \in \{1, \dots, N\}$ and implies that $\alpha(p) = N + 1 - p$. The upper and lower bounds for this case are respectively given by

$$\begin{aligned} \|G - \tilde{G}_{2q}\|_{\mathcal{L}_2[0,T],i} &\geq \frac{T}{2} \left(\cos\left(\frac{\pi(q+1)}{2(N+1)}\right) + \left(\cos\left(\frac{\pi(q+1)}{2(N+1)}\right)\right)^{-1} \right) \\ &= \frac{NT}{\pi} \left(1 - \frac{\pi^2(q+1)^2}{4N^2} + \mathcal{O}\left(\left(\frac{q+1}{N}\right)^4\right) \right), \end{aligned} \quad (44)$$

and

$$\begin{aligned} \|G - \tilde{G}_{2q}\|_{\mathcal{L}_2[0,T],i} &\leq \frac{eT}{2} \left(\cos\left(\frac{\pi(q+1)}{2(N+1)}\right) + \left(\cos\left(\frac{\pi(q+1)}{2(N+1)}\right)\right)^{-1} \right) \\ &= \frac{eNT}{\pi} \left(1 - \frac{\pi^2(q+1)^2}{4N^2} + \mathcal{O}\left(\left(\frac{q+1}{N}\right)^4\right) \right). \end{aligned} \quad (45)$$

This system is rather pathological since any good approximant must have $q \propto N$, as seen in equation (44). It is impossible for the error to be

made small unless q is of the same order as N . That q must scale as N implies that this system does not admit the same nice reductions as the previous example. Recall that for the previous example the relative error vanishes as $N \rightarrow \infty$ as long as $q \propto N^\delta$ for any δ such that $0 < \delta < 1$. Thus, decent reductions must retain far more states than the previous example. Despite this pathology, the appropriate reductions project out the slower modes. Since the same \mathbf{U}_d may be used as before (i.e. essentially a Fourier transform), the coarse graining keeps the small distance behavior (fast modes) and projects out the rest. For this system, high-frequency modes are more easily amplified, which explains the importance of including those modes in the approximate response.

• **The layered and random chains**

When \mathbf{U}_d is not a Fourier transform then these amenable dispersion relations are not guaranteed. Without such relations, modal reduction is not necessarily equivalent to local coarse graining. For example, consider a system with uniform masses and spring constants that under a unitary change of basis has the same $\mathbf{\Omega}^2$ as in (40) but without the spatial configuration of the linear chain (see Figure 6).

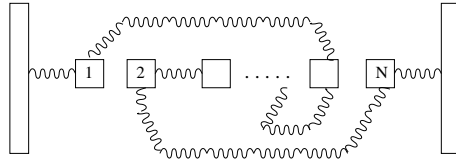


Figure 6: A spatially heterogeneous chain of linear oscillators. This is an example where spatially local coarse graining breaks down.

This system is an oscillator system with nonlocal interactions and a spatial Fourier transform will not diagonalize $\mathbf{\Omega}$. For this system, the appropriate reduction again would be a modal reduction since \mathbf{B} and \mathbf{C} only differ from \mathbf{I} by a unitary transformation. The exceptional thing about this example is that modal reduction lumps together oscillators that are far apart yet directly connected to each other. Consequently, it is not a local coarse graining. Although this system has the same characteristic frequencies and HSV as the homogeneous linear chain, long range interactions disrupt the validity of local coarse graining. Despite the artificial nature of this example, it illustrates the relationship between heterogeneity, non-locality, and long range interactions. Frustration, induced by competing interactions, also exemplifies these connections.

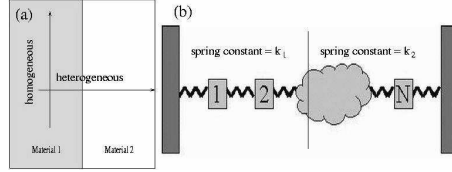


Figure 7: (a) A layered medium. (b) A layered chain of linear oscillators.

The scenario above is analogous to what happens in layered systems, as depicted in Figure 7. The material is homogeneous along one the vertical direction while it is heterogeneous in the other direction (transverse direction). The importance of such examples cannot be overemphasized, for they imply that the common practice of local coarse graining will not always apply to heterogeneous systems¹². Figure 8(a) depicts the HSV for a one dimensional layered harmonic chain, a variant of the scenario depicted in Figure 7. The spring constants are taken to be 0.125 on one side and 0.375 on the other. The HSV are distributed similarly to those of the homogeneous chain, as seen by comparing Figures 5(a) and 8(a) or by inspection of Figure 10(a). However, upon comparing Figures 5(b) and 8(b), the frequencies are quite different. Additionally, the transformation that diagonalizes Ω does not behave like a Fourier transform. Consequently, the appropriate coarse graining for this system is nonlocal.

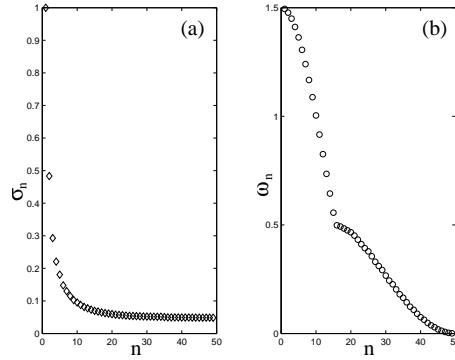


Figure 8: (a) A plot of the ordered HSV for the layered, harmonic oscillator chain. The HSV are plotted for $T \propto N^2$ where $N = 49$. The spring constant on one side is taken to be 0.125 one side and 0.375 on the other. (b) A plot of the frequencies for the same system.

When the spring constants are uniformly, randomly sampled from the interval $[0.125, 0.375]$, somewhat surprisingly, the HSV are distributed al-

¹²Under reasonably restrictive assumptions about the nature of there heterogeneities, the theory of homogenization allows one to effectively locally coarse grain an inhomogeneous system.

most identically to those of the homogeneous chain. As in the case of the layered chain, the frequencies of the random chain are different from those of the homogeneous one. Just as in the previous case, the coarse grainings for this system are nonlocal. In each case, when there is greater variation in the values of k , the distribution of HSV start to vary more from the purely homogeneous case.

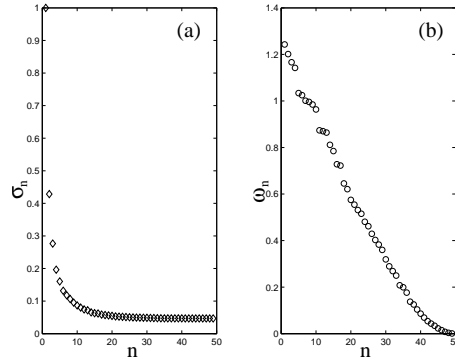


Figure 9: (a) A plot of the ordered HSV for the harmonic oscillator chain with uniformly sampled random springs. The spring constants are sampled from the interval $[0.125, 0.375]$. The HSV are plotted for $T \propto N^2$ where $N = 49$. (b) A plot of the frequencies for the same system.

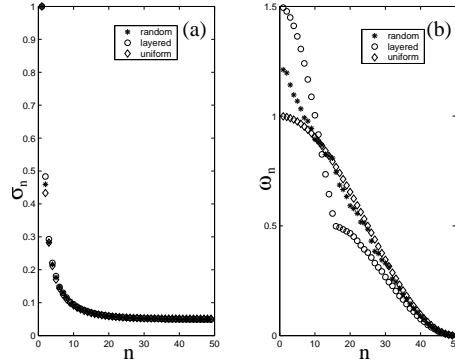


Figure 10: (a) A comparative plot of the ordered HSV for the different oscillator chains. The HSV are plotted for $T \propto N^2$ where $N = 49$. (b) Plots of the frequencies for the different oscillator chains.

4 Conclusions and Future Directions

Attempting to approximate systems by only considering their relevant details is not new in physics. For instance, resumming Feynman diagrams corresponding to prevalent physical processes attempts to do this. Such methods fail since they are not systematic. This is the novelty of this work. Not only does it provide a systematic way of determining how to coarse grain an arbitrary (linear) system, it also establishes how to implement the coarse graining in an algorithmic fashion. Furthermore, it is complementary to both the renormalization group (RG) [30, 31, 32] and the projection-operator formalism because it removes much of the ambiguity in coarse graining. Additionally, the Hankel methods can be used for arbitrary linear systems, not simply for generalized Hamiltonian systems. However, for general systems, the gramians are not guaranteed to take such simple forms.

This paper also answers an important question that was raised by Harle and Brun [10]. In that work, both the quantum and classical aspects of the harmonic chain (on a ring) were investigated. In particular, connections were made between different coarse grainings and the determinacy of the coarsened equations of motion (in the classical case) and also between different coarse grainings and decoherence (in the quantum case). They conjectured that local coarse graining led to more deterministic equations of motion for the coarsened degrees of freedom than nonlocal coarse graining, at least when the fast-mode initial conditions are thermally distributed. The induced noise for the locally-coarsened description was less than that for the nonlocal one. However, as was acknowledged in their work, the coarse grainings that were investigated constituted a set of measure zero of all the possible coarse grainings. This paper extends that work by considering arbitrary coarse grainings and more general quadratic Hamiltonians than just the harmonic chain. For the homogeneous harmonic chain with $2\sqrt{\frac{k}{m}} \leq 1$, we confirm that local coarse graining induces less noise than nonlocal coarse graining. Additionally, we establish that this conclusion does not generalize to arbitrary oscillator systems. In fact, we have shown that this relationship is contingent on the dispersion relation and how the HSV depend on the normal-mode frequencies. Consequently, for a different oscillator system, it is possible that nonlocal coarse grainings will yield the most deterministic equations of motion.

There are many theoretical directions in which this work can be taken, however, the greatest pool of problems are those that relate to physically-motivated models. The methods introduced here should be quite useful when applied to any number of physical systems where local coarse graining fails. For instance, inhomogeneous systems like layered or disordered

systems are prime nontrivial candidates. Additionally, this work is ideally suited for nonequilibrium systems. In particular, since it identifies the degrees of freedom that seem both most “excitable” and “observable”, it may be appropriate for revealing the true nature of effective temperatures [11]. For granular systems, this would be a big step towards identifying the importance of such mysterious quantities as the granular temperature and the free volume. Accordingly, it is in these directions, among others, that future work using these methods should be taken.

Acknowledgments

The author thanks Professors J. Hartle and I. Mezic for the conversations that culminated into this paper. Special thanks are also due to C. Maloney for his many questions and criticisms of this work. This work has also benefited from comments by Professor D. Cai. Lastly, the encouragements and suggestions from K. Reynolds and Professor J. Carlson are greatly appreciated and have been crucial to the completion of this work. This work was supported by the David and Lucile Packard Foundation, NSF Grant No. DMR-9813752, and EPRI/DoD through the Program on Interactive Complex Networks.

A Infinite time horizon results for finite time horizon problems

Approximating conservative linear systems over an infinite time horizon inevitably leads to divergences. This may be understood from the fact that the gramians become unbounded due to the infinite time horizon. A standard way to regulate this divergence is by approximating the system over a finite time horizon. Alternatively, the system can be exponentially discounted and considered over an infinite time horizon.

In this appendix we express the upper and lower bounds for the approximation of the input-output operator over a finite time horizon in terms of exponentially-discounted infinite-time-horizon Hankel singular values. Although this analysis is only applied to conservative systems, we find the bounds for arbitrary finite dimensional systems that admit LTI, causal realizations. Given a system realization $(\mathbf{A}, \mathbf{B}, \mathbf{C})$, we denote the input-output operator and its order r approximant respectively by G and \tilde{G}_r . Similarly, for the exponentially discounted system (i.e. with system matrix $-a\mathbf{I} + \mathbf{A}$), the input-output operator and its approximant are denoted by $G^{(a)}$ and $\tilde{G}_r^{(a)}$, respectively. Additionally, the finite time horizon HSV are given by

$\sigma_1 \geq \sigma_2 \geq \dots \geq \sigma_n$ while the infinite time horizon singular values are given by $\sigma_1(a) \geq \sigma_2(a) \geq \dots \geq \sigma_n(a)$.

Equation (19) as it is stated is equally valid for infinite or finite time horizons. However, we intend to relate $\|G - \tilde{G}_r\|_{\mathcal{L}_2[0,T],i}$ to the singular values $\{\sigma_i(a) : 1 \leq i \leq n\}$. The following new theorem establishes the relation of interest.

Theorem A.0.1 (Lower Bound) Given a LTI, causal system G with n dimensional minimal realization $(\mathbf{A}, \mathbf{B}, \mathbf{C})$. If there exists an “ a ” such that $-a\mathbf{I} + \mathbf{A}$ is a stable system matrix then for any order r (or less) approximant \tilde{G}_r

$$\|G - \tilde{G}_r\|_{\mathcal{L}_2[0,T],i} \geq (1 - e^{-2aT} \|e^{\mathbf{A}^\dagger T} e^{\mathbf{A}T}\|_{\mathbb{C}^n,i}) \sigma_{r+1}(a)$$

Proof:

Since the Hankel operator is simply a projection of the original input output operator we initially trivially find for an arbitrary \tilde{G}_r ,

$$\|G - \tilde{G}_r\|_{\mathcal{L}_2[0,T],i} \geq \|\Gamma_G - \Gamma_{\tilde{G}_r}\|_{\mathcal{L}_2[0,T],i} \geq \|\Gamma_G - \mathcal{K}_r\|_{\mathcal{L}_2[0,T],i}, \quad (46)$$

where \mathcal{K}_r is an arbitrary rank r operator that is not restricted to be of Hankel form. The last inequality arises because it is known that $\|\Gamma_G - \Gamma_{\tilde{G}_r}\|_{\mathcal{L}_2[0,T],i} \geq \sigma(\Gamma_G)$ and equality is not always possible since $\Gamma_{\tilde{G}_r}$ is of Hankel form. However, equality is achievable for an arbitrary operator \mathcal{K}_r .

The primary nontrivial step in this proof requires the observation that the each of the eigenvalues of the balanced gramian, $\bar{W}^{(a)}$, associated to $\Gamma_{G^{(a)}} = \Gamma^{(a)}$ are decreasing functions of a . This can be seen by noting that for any vector $\zeta \in \mathbb{R}^n$ and for $b < a$,

$$\left\langle \zeta, \left(\bar{W}^{(b)} - \bar{W}^{(a)} \right) \zeta \right\rangle \geq 0. \quad (47)$$

This means that $\sigma_k(a) \leq \sigma_k(b)$ for $a > b$. From this observation it is then follows that

$$\|\Gamma_G - \mathcal{K}_r\|_{\mathcal{L}_2[0,T],i} \geq \|\Gamma^{(a)} - \tilde{\mathcal{K}}_r\|_{\mathcal{L}_2[0,T],i}. \quad (48)$$

Then using that for any two bounded linear operators, \mathcal{A} and \mathcal{B} , in the induced norm $\|\mathcal{A}\mathcal{B}\| \leq \|\mathcal{A}\| \|\mathcal{B}\|$ and that

$$\|e^{\mathbf{A}T}\|_{\mathbb{C}^n,i} = \|e^{\mathbf{A}^\dagger T} e^{\mathbf{A}T}\|_{\mathbb{C}^n,i}^{1/2}, \quad (49)$$

we finally obtain

$$\begin{aligned} \|\Gamma^{(a)} - \tilde{\mathcal{K}}_r\|_{\mathcal{L}_2[0,T],i} &\geq \|\Gamma^{(a)} - \tilde{\mathcal{K}}_r\|_{\mathcal{L}_2[0,\infty],i} - \|\Gamma^{(a)} - \tilde{\mathcal{K}}_r\|_{\mathcal{L}_2[T,\infty],i} \\ &\geq (1 - e^{-2aT} \|e^{\mathbf{A}^\dagger T} e^{\mathbf{A}T}\|_{\mathbb{C}^n,i}) \sigma_{r+1}(a). \end{aligned} \quad (50)$$

Hence we arrive at the desired result,

$$\|G - \tilde{G}_r\|_{\mathcal{L}_2[0,T],i} \geq (1 - e^{-2aT} \|e^{\mathbf{A}^\dagger T} e^{\mathbf{A}T}\|_{\mathbb{C}^n,i}) \sigma_{r+1}(a). \quad (51)$$

In the case where \mathbf{A} has no Jordan blocks the above result simplifies to

$$\|G - \tilde{G}_r\|_{\mathcal{L}_2[0,T],i} \geq (1 - e^{2T \max \operatorname{Re} \lambda(-a\mathbf{I} + \mathbf{A})}) \sigma_{r+1}(a). \quad (52)$$

□

This lower bound is completely consistent with (19) for stable systems. Although we only use the upper bound in determining the relative error, we include it in the following. Recall from equation (23) that the upper bound is only valid for stable systems (for infinite time). In fact, it is almost exclusively proven for stable systems in the literature. The following upper bounds, valid for finite time horizon, are taken from [1].

Theorem A.0.2 (Upper Bound) Given a LTI, causal system G with n dimensional minimal realization $(\mathbf{A}, \mathbf{B}, \mathbf{C})$, if “ a ” is such that $-a\mathbf{I} + \mathbf{A}$ is a stable system matrix and $\|G^{(a)}\|_{\mathcal{L}_2,i} < \gamma$, then:

$$\|G\|_{\mathcal{L}_2[0,T],i} < \gamma e^{aT}$$

Proof: This results follows from the differential version of the bounded real lemma. For details refer to [1].

□

We already know from equation (23) how to obtain an upper bound for the approximation error, $\|G^{(a)} - \tilde{G}_r^{(a)}\|_{\mathcal{L}_2,i}$. We combine this fact with Theorem A.0.2 to obtain the following corollary.

Corollary A.0.3 (Upper Bound) Given a LTI, causal system G with n dimensional minimal realization $(\mathbf{A}, \mathbf{B}, \mathbf{C})$, if “ a ” is such that $-a\mathbf{I} + \mathbf{A}$ is a stable system matrix then there exists an order r input-output operator, \tilde{G}_r obtained by balanced truncation such that

$$\|G - \tilde{G}_r\|_{\mathcal{L}_2[0,T],i} < 2e^{aT} \sum_{j=1}^k \sigma_{i_j}^{\text{dist}}(a),$$

where $\sigma_{i_j}^{\text{dist}}(a)$, $1 \leq j \leq k$ are the distinct infinite time horizon HSV from the set $\{\sigma_{r+1}(a), \dots, \sigma_n(a)\}$.

To be precise, an algorithm to obtain \tilde{G}_r is as follows. First find the realization for $\tilde{G}_r^{(a)}$ by truncating the balanced realization of $(-a\mathbf{I} + \mathbf{A}, \mathbf{B}, \mathbf{C})$. Denote the resulting realization by $(\mathbf{A}_r, \mathbf{B}_r, \mathbf{C}_r)$. A realization for \tilde{G}_r is then just $(a\mathbf{I} + \mathbf{A}_r, \mathbf{B}_r, \mathbf{C}_r)$.

B Calculation of the Gramians

In this appendix we intend to calculate the balanced form of the gramians for oscillator systems (i.e. of systems of the form found in equation (25)). This entails calculating the damped (exponentially discounted) gramians:

$$\begin{aligned}\mathbf{W}_c^{(a)} &= \int_0^\infty e^{-2at} e^{\mathbf{A}t} e^{\mathbf{A}^\dagger t} dt \\ \mathbf{W}_o^{(a)} &= \int_0^\infty e^{-2at} e^{\mathbf{A}^\dagger t} e^{\mathbf{A}t} dt\end{aligned}\quad (53)$$

However, first let us introduce the following notations and conventions. Recall that any matrix, \mathbf{S} , may be expressed in terms of the canonical matrix units, \mathbf{e}_{ij} . In other words,

$$\mathbf{S} = \sum_{i,j} S_{ij} \mathbf{e}_{ij}$$

where each S_{ij} is just a complex number. For instance, in the case of 2×2 matrices,

$$\mathbf{e}_{12} = \begin{bmatrix} 0 & 1 \\ 0 & 0 \end{bmatrix}$$

Additionally, for this section, $\mathbf{Q} = \begin{bmatrix} 0 & 1 \\ -1 & 0 \end{bmatrix}$. Lastly, we frequently use the algebraic tensor product, \otimes ¹³. For instance, suppose

$$\mathbf{A} = \begin{bmatrix} A_{11} & A_{12} \\ A_{21} & A_{22} \end{bmatrix}$$

then

$$\mathbf{A} \otimes \mathbf{B} = \begin{bmatrix} A_{11}\mathbf{B} & A_{12}\mathbf{B} \\ A_{21}\mathbf{B} & A_{22}\mathbf{B} \end{bmatrix}$$

First note that if we define

$$\mathbf{R} = \mathbf{e}_{11} \otimes \Omega^{-1/2} + \mathbf{e}_{22} \otimes \Omega^{1/2} \quad (54)$$

then easily it follows that

$$\begin{aligned}\mathbf{A} &= \mathbf{e}_{12} \otimes \mathbf{I} - \mathbf{e}_{21} \otimes \Omega^2 = \begin{bmatrix} 0 & \mathbf{I} \\ -\Omega^2 & 0 \end{bmatrix} \\ \xrightarrow{\mathbf{R}} \mathbf{R}^{-1} \mathbf{A} \mathbf{R} &= \mathbf{Q} \otimes \Omega = \begin{bmatrix} 0 & \Omega \\ -\Omega & 0 \end{bmatrix}\end{aligned}\quad (55)$$

From this, one then finds that

$$\begin{aligned}\mathbf{W}_c^{(a)} &= \mathbf{R} \int_0^\infty e^{-2at} e^{\mathbf{Q} \otimes \Omega t} \mathbf{R}^{-1} \mathbf{R}^{-1} e^{-\mathbf{Q} \otimes \Omega t} dt \mathbf{R} \\ &= \mathbf{R} \int_0^\infty e^{-2at} e^{\mathbf{Q} \otimes \Omega t} \begin{bmatrix} \Omega & 0 \\ 0 & \Omega^{-1} \end{bmatrix} e^{-\mathbf{Q} \otimes \Omega t} dt \mathbf{R}\end{aligned}\quad (56)$$

¹³Often referred to as the dyadic product.

However, using that $e^{\mathbf{Q} \otimes \Omega t} = \mathbf{I} \otimes \cos \Omega t + \mathbf{Q} \otimes \sin \Omega t$ we finally arrive at

$$\begin{aligned}
\mathbf{W}_c^{(a)} &= \mathbf{R} \int_0^\infty e^{-2at} \times \\
&\left[\begin{array}{cc} \Omega \cos^2 \Omega t + \Omega^{-1} \sin^2 \Omega t & \frac{1}{2} \Omega^{-1} (\Omega^{-1} - \Omega) \frac{d}{dt} \sin^2 \Omega t \\ \frac{1}{2} \Omega^{-1} (\Omega^{-1} - \Omega) \frac{d}{dt} \sin^2 \Omega t & \Omega^{-1} \cos^2 \Omega t + \Omega \sin^2 \Omega t \end{array} \right] dt \mathbf{R} \\
&= \frac{1}{4a} \mathbf{R} \left[\begin{array}{cc} \Omega + \Omega^{-1} & 0 \\ 0 & \Omega + \Omega^{-1} \end{array} \right] \mathbf{R} + \frac{1}{4a} \mathbf{R} \times \\
&\left[\begin{array}{cc} -a^2 \Omega^{-1} (\mathbf{I} - \Omega^2) (a^2 \mathbf{I} + \Omega^2)^{-1} & a (\mathbf{I} - \Omega^2) (a^2 \mathbf{I} + \Omega^2)^{-1} \\ a (\mathbf{I} - \Omega^2) (a^2 \mathbf{I} + \Omega^2)^{-1} & a^2 \Omega^{-1} (\mathbf{I} - \Omega^2) (a^2 \mathbf{I} + \Omega^2)^{-1} \end{array} \right] \mathbf{R}.
\end{aligned} \tag{57}$$

Similarly for the observability gramian we obtain

$$\begin{aligned}
\mathbf{W}_o^{(a)} &= \frac{1}{4a} \mathbf{R}^{-1} \left[\begin{array}{cc} \Omega + \Omega^{-1} & 0 \\ 0 & \Omega + \Omega^{-1} \end{array} \right] \mathbf{R}^{-1} + \frac{1}{4a} \mathbf{R}^{-1} \times \\
&\left[\begin{array}{cc} a^2 \Omega^{-1} (\mathbf{I} - \Omega^2) (a^2 \mathbf{I} + \Omega^2)^{-1} & a (\mathbf{I} - \Omega^2) (a^2 \mathbf{I} + \Omega^2)^{-1} \\ a (\mathbf{I} - \Omega^2) (a^2 \mathbf{I} + \Omega^2)^{-1} & -a^2 \Omega^{-1} (\mathbf{I} - \Omega^2) (a^2 \mathbf{I} + \Omega^2)^{-1} \end{array} \right] \mathbf{R}^{-1}.
\end{aligned} \tag{58}$$

From equations (57) and 58 it follows after using \mathbf{U}_d to diagonalize Ω and taking the small “ a ” limit that the balanced gramian, without ordered eigenvalues, is given by

$$\bar{\mathbf{W}}_c = \bar{\mathbf{W}}_o = \frac{1}{4a} \left[\begin{array}{cc} \Lambda_\Omega + \Lambda_\Omega^{-1} + \mathcal{O}(a^2) & \mathcal{O}(a) \\ \mathcal{O}(a) & \Lambda_\Omega + \Lambda_\Omega^{-1} + \mathcal{O}(a^2) \end{array} \right].$$

C Restrictions on the time horizon/exponential discounting

C.1 Relevant matrix perturbation

We start with a matrix \mathbf{L}_ϵ of the form,

$$\mathbf{L}_\epsilon = \begin{pmatrix} \mathbf{M} & \epsilon \mathbf{N} \\ \epsilon \mathbf{N} & \mathbf{M} \end{pmatrix}. \tag{59}$$

The question we intend to address is, how do the ϵ terms perturb the spectrum of \mathbf{L}_0 .

$$\begin{aligned}
\det(\lambda \mathbf{I} - \mathbf{L}_\epsilon) &= \det \begin{pmatrix} \lambda \mathbf{I} - \mathbf{M} & -\epsilon \mathbf{N} \\ -\epsilon \mathbf{N} & \lambda \mathbf{I} - \mathbf{M} \end{pmatrix} \\
&= \det \begin{pmatrix} \lambda \mathbf{I} - \mathbf{M} & -\epsilon \mathbf{N} \\ 0 & \lambda \mathbf{I} - \mathbf{M} - \epsilon^2 \mathbf{N} (\lambda \mathbf{I} - \mathbf{M})^{-1} \mathbf{N} \end{pmatrix} \\
&= \det(\lambda \mathbf{I} - \mathbf{M}) \det(\lambda \mathbf{I} - \mathbf{M} - \epsilon^2 \mathbf{N} (\lambda \mathbf{I} - \mathbf{M})^{-1} \mathbf{N}) \\
&= (\det(\lambda \mathbf{I} - \mathbf{M}))^2 \det(\mathbf{I} - \epsilon^2 ((\lambda \mathbf{I} - \mathbf{M})^{-1} \mathbf{N})^2)
\end{aligned} \tag{60}$$

However, recall that given an invertible matrix \mathbf{P} ,

$$\mathbf{P}^{-1} = (\det(\mathbf{P}))^{-1} \text{adj}(\mathbf{P}), \quad (61)$$

where adj is the formal matrix adjoint. Combining (61) with the fact that $\epsilon \ll 1$, we obtain:

$$\det(\lambda \mathbf{I} - \mathbf{L}_\epsilon) \approx \left(\det(\lambda \mathbf{I} - \mathbf{M}) \right)^2 - \epsilon^2 \text{Tr} \left((\text{adj}(\lambda \mathbf{I} - \mathbf{M}) \mathbf{N})^2 \right). \quad (62)$$

Now, let us evaluate the above at an eigenvalue of L_ϵ that is ‘‘near’’ an eigenvalue of L_0 . Thus, $\lambda = \lambda_0 + \hat{\lambda}(\epsilon)$, where λ_0 is an eigenvalue of L_0 and $\hat{\lambda}(\epsilon) \rightarrow 0$ as $\epsilon \rightarrow 0$. First consider the transformation \mathbf{U} that has the property that

$$\mathbf{U}^{-1} \mathbf{M} \mathbf{U} = \begin{pmatrix} \tilde{\mathbf{M}} & 0 \\ 0 & \lambda_0 \mathbf{I}_{r \times r} \end{pmatrix}, \quad (63)$$

where $r \geq 1$. From this we find

$$\begin{aligned} \det(\lambda_0 \mathbf{I} - \mathbf{M} + \hat{\lambda}(\epsilon) \mathbf{I}) &= \hat{\lambda}^r(\epsilon) \det(\lambda_0 \mathbf{I} - \tilde{\mathbf{M}}) \det(\mathbf{I} + \hat{\lambda}(\epsilon) (\lambda_0 \mathbf{I} - \tilde{\mathbf{M}})^{-1}) \\ &= \hat{\lambda}^r(\epsilon) \det(\lambda_0 \mathbf{I} - \tilde{\mathbf{M}}) \left[1 + \hat{\lambda}(\epsilon) (\det(\lambda_0 \mathbf{I} - \tilde{\mathbf{M}}))^{-1} \text{Tr}(\text{adj}(\lambda_0 \mathbf{I} - \tilde{\mathbf{M}})) \right] \\ &+ \mathcal{O}(\hat{\lambda}^{r+2}(\epsilon)) = \hat{\lambda}^r(\epsilon) \det(\lambda_0 \mathbf{I} - \tilde{\mathbf{M}}) + \hat{\lambda}^{r+1}(\epsilon) \text{Tr}(\text{adj}(\lambda_0 \mathbf{I} - \tilde{\mathbf{M}})) \\ &+ \mathcal{O}(\hat{\lambda}^{r+2}(\epsilon)). \end{aligned} \quad (64)$$

Combining (62) and (64), results in

$$\begin{aligned} \det(\lambda \mathbf{I} - \mathbf{L}_\epsilon) &= \hat{\lambda}^{2r}(\epsilon) (\det(\lambda_0 \mathbf{I} - \tilde{\mathbf{M}}))^2 \\ &- \epsilon^2 \text{Tr} \left((\text{adj}(\lambda_0 \mathbf{I} - \mathbf{M}) \mathbf{N})^2 \right) + \mathcal{O}(\max\{\hat{\lambda}^{2r+1}(\epsilon), \epsilon^2 \hat{\lambda}(\epsilon)\}) = 0. \end{aligned} \quad (65)$$

This naively suggests that $|\hat{\lambda}(\epsilon)| \sim \epsilon^{1/r}$. However, unless \mathbf{M} has Jordan blocks, $\text{adj}(\lambda \mathbf{I} - \mathbf{M})|_{\lambda=\lambda_0} = 0$. We will consider \mathbf{M} to be diagonalizable, in order to discern the behavior of $\hat{\lambda}(\epsilon)$. Thus, in the basis where $\mathbf{M} \rightarrow \mathbf{\Lambda}_\mathbf{M}$ (i.e. the basis where \mathbf{M} is diagonal), the following holds:

$$\frac{d^p}{d\lambda^p} \text{adj}(\lambda \mathbf{I} - \mathbf{\Lambda}_\mathbf{M})|_{\lambda=\lambda_0} = 0 \quad \text{For all } p < r - 1. \quad (66)$$

In this case, we find

$$\begin{aligned} \text{adj}(\lambda \mathbf{I} - \mathbf{\Lambda}_\mathbf{M})|_{\lambda=\lambda_0+\hat{\lambda}(\epsilon)} &= \frac{\hat{\lambda}^{r-1}(\epsilon)}{(r-1)!} \frac{d^{r-1}}{d\lambda^{r-1}} \text{adj}(\lambda \mathbf{I} - \mathbf{\Lambda}_\mathbf{M}) + \mathcal{O}(\hat{\lambda}^r(\epsilon)) \\ &= \frac{\hat{\lambda}^{r-1}(\epsilon)}{(r-1)!} \det(\lambda_0 \mathbf{I} - \tilde{\mathbf{M}}) \begin{pmatrix} 0 & 0 \\ 0 & \mathbf{I}_{r \times r} \end{pmatrix} + \mathcal{O}(\hat{\lambda}^r(\epsilon)). \end{aligned} \quad (67)$$

Combining (65) and (67) and provided that there exists a transformation \mathbf{V} such that $\mathbf{V}^{-1}\mathbf{M}\mathbf{V} = \mathbf{\Lambda}_M$ and $\mathbf{V}^{-1}\mathbf{N}\mathbf{V} = \tilde{\mathbf{N}}$ we obtain the result

$$\begin{aligned} \det(\lambda\mathbf{I} - \mathbf{L}_\epsilon) &= \hat{\lambda}^{2r}(\epsilon) (\det(\lambda_0\mathbf{I} - \tilde{\mathbf{M}}))^2 - \frac{1}{((r-1)!)^2} \epsilon^2 \hat{\lambda}^{2r-2}(\epsilon) \text{Tr}(\tilde{\mathbf{N}}_{22})^2 \\ &\quad + \mathcal{O}(\max\{\hat{\lambda}^{2r+1}(\epsilon), \epsilon^2 \hat{\lambda}^{2r-1}(\epsilon)\}) = 0, \end{aligned} \quad (68)$$

where $\tilde{\mathbf{N}}_{22}$ is an $r \times r$ matrix that comes from

$$\tilde{\mathbf{N}} = \begin{pmatrix} \tilde{\mathbf{N}}_{11} & \tilde{\mathbf{N}}_{12} \\ \tilde{\mathbf{N}}_{21} & \tilde{\mathbf{N}}_{22} \end{pmatrix}. \quad (69)$$

Hence we finally arrive at

$$|\hat{\lambda}_i(\epsilon)| = \frac{\epsilon}{(r-1)!} \sqrt{|\text{Tr}(\tilde{\mathbf{N}}_{22})^2|} + \mathcal{O}(\epsilon^2). \quad (70)$$

C.2 Consequences: Results put in context

For $r = 1$ and $\tilde{\mathbf{N}}$ is Hermitian, (70) directly implies that the i^{th} eigenvalue of \mathbf{M} is perturbed as

$$|\hat{\lambda}_i(\epsilon)| = \epsilon |\tilde{\mathbf{N}}_{ii}| + \mathcal{O}(\epsilon^2) \leq \epsilon \|\mathbf{N}\|_\infty + \mathcal{O}(\epsilon^2). \quad (71)$$

This provides an upper bound on how the perturbation shifts the spectrum of the unperturbed matrix.

From Appendix B, we can make the following associations; $\epsilon = a$, $\mathbf{M} = \mathbf{\Lambda}_\Omega + \mathbf{\Lambda}_\Omega^{-1}$, and $\mathbf{N} = \mathbf{\Lambda}_\Omega^{-2} - \mathbf{I}$. Our objective is to roughly determine the size of “ a ” such that the ordering of the Hankel singular values are preserved. As in Section 3.1, given that $\lambda_j(\mathbf{\Omega}) \leq \lambda_k(\mathbf{\Omega})$ for all $j < k$, let α be a permutation such that $\lambda_{\alpha(j)}(\mathbf{\Omega}) + \lambda_{\alpha(j)}^{-1}(\mathbf{\Omega}) \leq \lambda_{\alpha(k)}(\mathbf{\Omega}) + \lambda_{\alpha(k)}^{-1}(\mathbf{\Omega})$ for all $k < j$. Though it is somewhat conservative, the ordering about the i^{th} unperturbed Hankel singular value is guaranteed provided that

$$\begin{aligned} a \left(|\lambda_{\alpha(i)}^{-2} - 1| + |\lambda_{\alpha(i+1)}^{-2} - 1| \right) &\leq \lambda_{\alpha(i)}^{-1} + \lambda_{\alpha(i)} - \lambda_{\alpha(i+1)}^{-1} + \lambda_{\alpha(i+1)}, \\ a \left(|\lambda_{\alpha(i-1)}^{-2} - 1| + |\lambda_{\alpha(i)}^{-2} - 1| \right) &\leq \lambda_{\alpha(i-1)}^{-1} + \lambda_{\alpha(i-1)} - \lambda_{\alpha(i)}^{-1} + \lambda_{\alpha(i)}. \end{aligned} \quad (72)$$

It follows that the ordering of the HSV is guaranteed to be preserved provided that

$$a \leq \min_{1 \leq i \leq N-1} \frac{\lambda_{\alpha(i)}^{-1} + \lambda_{\alpha(i)} - \lambda_{\alpha(i+1)}^{-1} - \lambda_{\alpha(i+1)}}{|\lambda_{\alpha(i)}^{-2} - 1| + |\lambda_{\alpha(i+1)}^{-2} - 1|}. \quad (73)$$

References

- [1] M. Sznaier, A.C. Doherty, M. Barahona, J.C. Doyle, and H. Mabuchi, “A New Bound of the $\mathcal{L}_2[0, T]$ -Induced Norm and Applications to Model Reduction,” *Proceedings ACC* **2**, 1180 (2002).
- [2] M. Barahona, A.C. Doherty, M. Sznaier, H. Mabuchi, and J.C. Doyle, “Finite Horizon Model Reduction and the Appearance of Dissipation of Hamiltonian Systems,” *Proceedings of IEEE CDC* **4**, 4563 (2002).
- [3] Reynolds, et. al. (in preparation).
- [4] C. Rowley, (in preparation).
- [5] R. Zwanzig, “Nonlinear generalized langevin equations,” *J. Stat. Phys.* **9**, 215-220 (1973).
- [6] H. Mori, “Transport, collective motion, and Brownian motion,” *Prog. Theor. Phys.* **33**, 423-450 (1965).
- [7] H. Mori, “A continued-fraction representation of time-correlation functions,” *Prog. Theor. Phys.* **34**, 399 (1965).
- [8] G.W. Ford and M. Kac, “On the quantum langevin equation,” *J. Stat. Phys.* **46**, 803-810 (1987).
- [9] M. Gell-Mann and J. Hartle, “Classical equations for quantum systems,” *Phys. Rev. D* **47**, 3345-3382 (1993).
- [10] T. Brun and J. Hartle, “Classical dynamics of the quantum harmonic chain,” *Phys. Rev. D* **60**, 123503 (1999).
- [11] L.F. Cugliandolo, J. Kurchan, and L. Peliti, “Energy flow, partial equilibration, and effective temperatures in systems with slow dynamics,” *Phys. Rev. E* **55**, 3898-3914 (1997).
- [12] J.-P. Hansen and I.R. McDonald, *Theory of Simple Liquids*, 2nd Edition (Academic Press, San Diego, 1990).
- [13] N.G. van Kampen, *Stochastic Processes in Physics and Chemistry*, Revised and enlarged Edition (Elsevier, Amsterdam, 2001).
- [14] R. Kubo, M. Toda, N. Hashitsume, *Statistical Physics II*, 2nd Edition (Springer-Verlag, Berlin, 1991).
- [15] K. Glover, “All optimal Hankel-norm approximations of linear-multivariable systems and their L infinity-error bounds,” *Int. J. Control* **39**, 1115-1193 (1984).

- [16] A. Feintuch, *Robust Control Theory in Hilbert Space*, (Springer-Verlag, New York, 1998).
- [17] A. Böttcher and B. Silbermann, *Introduction to Large Truncated Toeplitz Matrices*, (Springer-Verlag, New York, 1999).
- [18] A. Böttcher and S.M. Grudsky, *Toeplitz Matrices, Asymptotic Linear Algebra, and Functional Analysis*, (Birkhäuser, Boston, 2000).
- [19] A. Böttcher and B. Silbermann, *Analysis of Toeplitz Operators*, (Springer-Verlag, New York, 1990).
- [20] G.E. Dullerud and F. Paganini, *A Course in Robust Control Theory*, (Springer-Verlag, New York, 2000).
- [21] V.V. Peller, *Hankel Operators and their Applications*, (Springer-Verlag, New York, 2003).
- [22] N.K. Nikolski, *Operators, Functions and Systems: An Easy Reading Volume I: Hardy, Hankel, and Toeplitz*, (American Mathematical Society, Providence, 2002).
- [23] J.R. Partington, *Interpolation, Identification, and Sampling*, (Oxford University Press, New York, 1997).
- [24] K. Zhou and J.C. Doyle, *Essentials of Robust Control*, (Prentice-Hall, New Jersey, 1998).
- [25] G. Vinnicombe, *Uncertainty and Feedback: \mathcal{H}_∞ Loop-Shaping and the ν -Gap Metric*, (Imperial College Press, Singapore, 2000).
- [26] S. Boyd, L. El Ghaoui, E. Feron, and V. Balakrishnan, *Linear Matrix Inequalities in System and Control Theory*, (SIAM, Philadelphia, 1994).
- [27] J.M.A. Scherpen, "Balancing for nonlinear-systems," *Syst. Contr. Lett.* **21**, 143-153 (1993).
- [28] J.M.A. Scherpen, "H-infinity balancing for nonlinear systems," *Int. J. Robust Nonlin. Contr.* **6**, 645-668 (1996).
- [29] J.M.A. Scherpen, "Minimality and local state decompositions of a nonlinear state space realization using energy functions," *IEEE Trans. Automat. Contr.* **45**, 2079-2086 (2000).
- [30] L.-Y. Chen, N. Goldenfeld, and Y. Oono, "Renormalization group and singular perturbations: Multiple scales, boundary layers, and reductive perturbation theory," *Phys. Rev. E* **54**, 376-394 (1996).

- [31] Y. Oono, “Renormalization and asymptotics,” *Int. J. Mod. Phys. B* **14**, 1327-1361 (2000).
- [32] K. Nozaki and Y. Oono, “Renormalization-group theoretical reduction,” *Phys. Rev. E* **63**, 046101 (2001).
- [33] N. Goldenfeld, *Lectures on Phase Transitions and the Renormalization Group*, (Perseus, Reading, MA, 1992).
- [34] A. Lesne, *Renormalization Methods*, (John Wiley & Sons, Chichester, UK, 1998).
- [35] J. Bricmont, A. Kupiainen, and R. Lefevre, “Renormalizing the renormalization group pathologies,” *Phys. Rep.* **348**, 5-31 (2001).
- [36] J. Bricmont, A. Kupiainen, and R. Lefevre, “Renormalization group pathologies and the definition of Gibbs states,” *Commun. Math. Phys.* **194**, 359-388 (1998).
- [37] J. Bricmont, A. Kupiainen, “Phase transition in the 3d random field Ising model,” *Commun. Math. Phys.* **116**, 539-572 (1988).